APPLICATION OF FLUORESCENT MELAMINE RESIN MICROSPHERES FOR USE AS A GEOTHERMAL TRACER

A THESIS SUBMITTED TO
THE GRADUATE SCHOOL OF NATURAL AND APPLIED SCIENCES
OF
MIDDLE EAST TECHNICAL UNIVERSITY

BY

MUSTAFA SALAR

IN PARTIAL FULFILLMENT OF THE REQUIREMENTS
FOR
THE DEGREE OF MASTER OF SCIENCE
IN
PETROLEUM AND NATURAL GAS ENGINEERING

AUGUST 2018

Approval of the Thesis:

APPLICATION OF FLUORESCENT MELAMINE RESIN MICROSPHERES FOR USE AS A GEOTHERMAL TRACER

Submitted by **MUSTAFA SALAR** in partial fulfillment of the requirements for the degree of **Master of Science in Petroleum and Natural Gas Engineering Department, Middle East Technical University** by,

Prof. Dr. Halil Kalıpçılar
Dean, Graduate School of **Natural and Applied Sciences** _____

Prof. Dr. Serhat Akın
Head of Department, **Petroleum and Natural Gas Eng.** _____

Prof. Dr. Serhat Akın
Supervisor, **Petroleum and Natural Gas Eng. Dept., METU** _____

Examining Committee Members:

Assoc. Prof. Çağlar Sınayuç
Petroleum and Natural Gas Engineering Dept., METU _____

Prof. Dr. Serhat Akın
Petroleum and Natural Gas Engineering Dept., METU _____

Asst. Prof. Tuna Eren
Petroleum and Natural Gas Engineering Dept.,
Izmir Katip Celebi University _____

Date: 14.08.2018

I hereby declare that all information in this document has been obtained and presented in accordance with academic rules and ethical conduct. I also declare that, as required by these rules and conduct, I have fully cited and referenced all material and results that are not original to this work.

Name, Last name: Mustafa Salar

Signature:

ABSTRACT

APPLICATION OF FLUORESCENT MELAMINE RESIN MICROSPHERES FOR USE AS A GEOTHERMAL TRACER

Salar, Mustafa

M.Sc., Department of Petroleum and Natural Gas Engineering

Supervisor: Prof. Dr. Serhat Akın

August, 2018, 94 pages

Tracer testing of flow between injection and production wells is an effective tool to map fluid flow pathways in a geothermal reservoir. Tracer concentration curves can be used to provide insight into projected thermal drawdown in the reservoir or thermal breakthrough of re-injected fluids, estimating inter-well volumes and flow geometries. Although radioactive tracers have been used in the past, many tracer tests now use chemical tracers that are less hazardous to handle. Fluorescent organic compounds such as fluorescein and rhodamine-B, other fluorescent compounds such as naphthalene sulfonates and dissolved inorganic solutes such as potassium iodide (KI) and potassium bromide can be used as geothermal tracers. Nano-micro colloids have been suggested as 'smart' geothermal tracers because of controlling parameters such as particle size. Tracer experiments were conducted using micro melamine resin rhodamine B particles with differing sizes ranging from 4 μm to 10 μm and conventional rhodamine B in a 2-D cross sectional model built from marble blocks that represents a low enthalpy liquid dominated geothermal reservoir. It has been observed that first arrival time of micro tracers was 4 times earlier than those observed in conventional rhodamine B tracer. The effect of injection rate, particle size and fracture geometry on recovery of micro particles was also investigated. It was found

that the recovery of the micro particles increased with increasing flow rate and the particle size has the inverse relation with particle recovery.

Keywords: Tracer, micro particles, rhodamine B, melamine resin

ÖZ

FLORESAN MELAMİN RESİN MİKROKÜRELERİNİN JEOTERMAL İZLEYİCİ OLARAK UYGULANMASI

Salar, Mustafa
Yüksek Lisans, Petrol ve Doğal Gaz Mühendisliği Bölümü
Tez Yöneticisi: Prof. Dr. Serhat Akın

Ağustos, 2018, 94 sayfa

Enjeksiyon ve üretim kuyuları arasındaki akışın izleyici testi, bir jeotermal rezervuardaki akış yollarını haritalamada etkili bir araçtır. İzleyici konsantrasyon eğrileri, rezervuarda projelendirilmiş termal düşüm veya yeniden enjekte edilen akışkanların ısıl geçişi hakkında fikir vermek için kullanılabilir; bunlar, kuyular arası hacimleri ve akış geometrilerini tahmin ederler. Geçmişte radyoaktif izleyiciler kullanılmış olmasına rağmen, birçok tracer testi artık ele alınması daha az tehlikeli olan kimyasal izleyicileri kullanmaktadır. Florescein ve Rodamin-B gibi florasan organik bileşikler, naftalin sülfonatlar, potasyum iyodür (KI) ve potasyum bromür gibi çözünmüş inorganik çözeltiler, jeotermal izleyiciler olarak kullanılabilir. Nano- mikro kolloidler, 'smart' jeotermal izleyiciler olarak önerilmiştir. İzleyici deneyleri, 4 μm ila 10 μm arasında değişen farklı boyutlara sahip mikro melamin reçine ve konvansiyonel rodamin B partikülleriyle düşük entalpili sıvı baskın jeotermal rezervuarı temsil eden 2-D kesit modelindeki mermer bloklarla yapılmıştır. Mikro izleyicilerin ilk varış zamanının gözlemlenen konvensiyonel Rodamin-B izleyicisinden 4 kat daha erken olduğu gözlenmiştir. Enjeksiyon akış oranı, partikül boyutu ve çatlak geometrisinin mikro partikül kurtarım oranına etkisi de araştırılmıştır. Enjeksiyon akış oranı arttıkça mikro partikül kurtarım oranının arttığı görülmüştür ayrıca mikro partikül boyutuyla

mikro partikül kurtarımı arasındada ters orantı olduğu görülmüştür.

Anahtar Kelimeler: İzleyiciler, Mikro Partiküller, Rodamin B, Melamin Reçinesi

ACKNOWLEDGEMENT

I would like to thank my thesis advisor Prof. Dr. Serhat Akın for his valuable encouragement and guidance throughout this study.

Special thanks to Naci Doğru and Murat Çalışkan for their effort in helping and encouraging me to pursue my goal.

Lastly, I would like to thank to Süher Salar who always support and encourage me.

TABLE OF CONTENTS

LIST OF FIGURES

FIGURES

LIST OF TABLES

TABLES

NOMENCLATURE

A = Area (m^2)

b = Block size (m)

C = Concentration (ppb)

Cexp = Experimental concentration (ppb)

Cr = Observed concentration (ppb)

Ct = Total concentration (ppb)

C_t = Transfer function

D = Dispersion coefficient

Dz = Axial dispersivity

Eapp(t) = The apparent residence time distribution

e_i = Flow contribution coefficient

FAT = First arrival time

J = Model parameter

K = Model parameter of uniform porous

m = Mass of tracer chemical (mg)

MAT= Mean arrival time

n = Number of flow channels in the fracture system

Pe_i = Peclet number of i^{th} flow channel

Q = Flow rate (ml/min)

R_i = Apparent fracture length (cm)

SAT = Second arrival time

t^* = The mean residence time (min)

t_b = Response start time (min)

t_r = The mean arrival time (min)

U = Heaviside step distribution

u_i = Velocity (cm min^{-1})

w = A ratio of transport along the fracture to transport out of the fracture

α_f = The rate of tracer interchange per unit fracture volume (ml/s)

α_m = The rate of tracer interchange per unit matrix volume (ml/s)

μm = Micrometer

CHAPTER 1

INTRODUCTION

The name of geothermal can be broken down to ‘Earth’ (Geo) and ‘Heat’ (Thermal) based on the Greek language. Geothermal energy is a renewable energy that is described as the heat energy of the earth. The heat of the earth produced by radioactive decay and the temperature of outer core- inner mantle line is about 3000 ^{o}C (Figure 1.1). Geothermal energy has been retrieved by humans and used in different places such as bathing, space heating and electricity production from paleolithic times to present day.

Geothermal energy is reliable, renewable and environmental friendly. Contrary to other renewable energy resources, geothermal energy meets most of energy demand. There are six identified geothermal systems; Magma, hydrothermal, geopressurized, hot dry rock, enhanced geothermal systems and waste heat [1]. Generally hydrothermal resources, which necessitate heat, fluid and permeability occurring in porous rock or fractures are used for production of geothermal energy however, the research about hot dry rock and enhanced geothermal systems have increased recently.

All modern geothermal projects include geothermal reinjection programs that started in the early 1970s both in low and high temperature reservoirs. Geothermal reinjection program is an effective way to waste-water disposal in addition to supply extra recharge to geothermal systems. Reinjection is a crucial part of sustainable and inclusive geothermal source management. Geothermal projects with reinjection programs have more advantages than without reinjection programs because,

reinjection supplies extra recharge and opposing action to pressure draw down as a result of production from reservoir rocks.

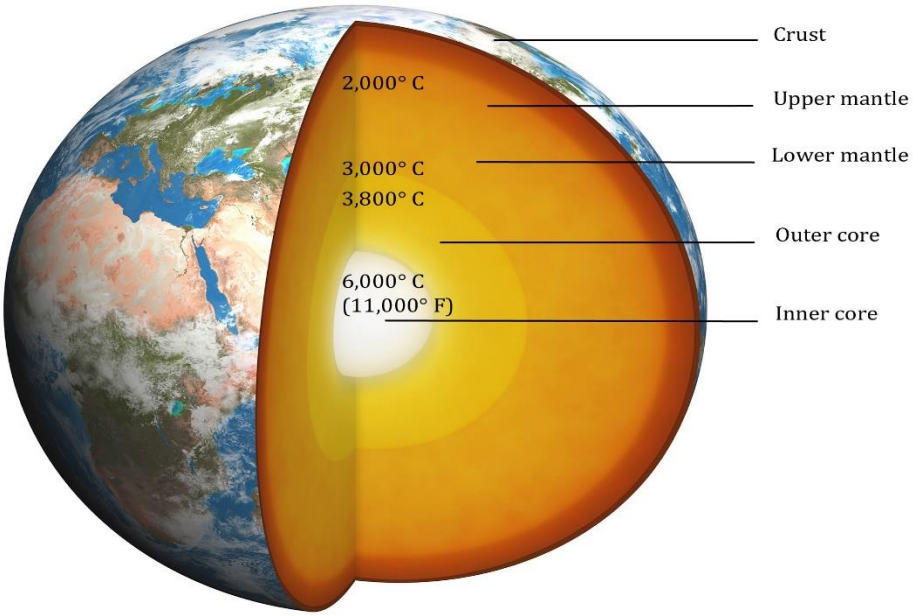

Figure 1.1 Depth and Temperature of Earth [2]

As opposed to benefits of reinjection, it may create some troublesome situations and problems. Production wells sometimes can become cool because of cold front breakthrough, short circulating and scaling in surface materials. Reinjection may have both adventageous and risky effects. Therefore, transport phenomena in the reservoir and reinjection fluid behaviour should be examined. For better understanding the reinjection fluid behaviour and prospering geothermal projects, tracer tests have become profoundly significant application in geothermal fields. Tracer tests supply information about flow paths and connections between production and reinjection wells. The cooling rate of production wells can be learned by reinjection of cooler liquid on the long run. Therefore, interwell tracer tests have made significant contributions for understanding the behavior of a reinjected cold fluid within the reservoir and to develope an optimal reinjection program to maximize energy production from a specific geothermal field.

Radioactive and chemical tracers have been used for many years in groundwater hydrology to study the fluid movement through porous media. In addition to test itself, a method or model to analyze the obtained test data is required.
Tracer tests in geothermal fields may include a backflow test (single well injection), a one well pair (production and injection) or include various injection and production wells. Mostly, tracer is injected in ‘‘slug’’ form in shortest time possible. There are three types of tracers used in geothermal systems: Liquid phase tracers, steam phase tracers and two phase tracers. These three types of tracers have been used many years for understanding the fluid behaviour and transport phenomena in through porous media in geothermal systems [3].

Conventional tracer substances are generally hydrophilic and as such will diffuse significantly within the porous media. Although conventional tracers can provide a wide range of information about flow paths and parameters such as dispersivity, fluid velocity, Peclet number etc. with developed flow models, they are still insufficient for detailed evaluation of transport system of the fractured rock. For example, it is difficult to evaluate the fracture aperture or matrix pore size with conventional tracer models. In addition, conventional tracers have a high tendency of diffusion into rock matrix, which causes high retention. However, micro particles are very useful because of their physical and chemical controlling properties (Figure 1.2). Therefore, nanoparticle and micro particles have been introduced to overcome the restrictions with conventional tracers in fractured rocks. Several studies have been published regarding the application of particle tracers in fractured rocks. Zhang et al. (2015) investigated DNA-tagged nanotracers, which were coated with silica nanoparticles for applicability in geothermal reservoirs [4]. They observed that silica nanoparticles showed good flow characteristics at high temperatures through porous media and these nanotracers were found to be viable for geothermal tracer applications. Rose et al. (2011), introduced colloidal nanocrystal quantum dots for quantitatively measuring the surface area of fractures within a geothermal and EGS reservoir [5]. They stated that the potential of modifying surface chemistry and diameter of quantum dots can be used as a tool for characterizing fracture surface areas. In this study, the transport of micro melamine resin rhodamine B-marked particles is investigated in a 2-D cross sectional low

enthalpy geothermal reservoir model built from marble blocks. Micro melamine resin particles are chosen because the particles are stable at temperature up to 300°C, surface of particles is hydrophilic, long term stability in aqueous media, the density of micro particles are higher than water density so these particles can easily enter the small fractures and digital filter fluorometer can detect micro melamine resin particles easily [6]. The flow models of conventional rhodamine B and micro melamine particles are studied to find out similarities and differences between them. We were also able to observe the recovery and retention of micro particles by controlling parameters such as particle size and injection rate.

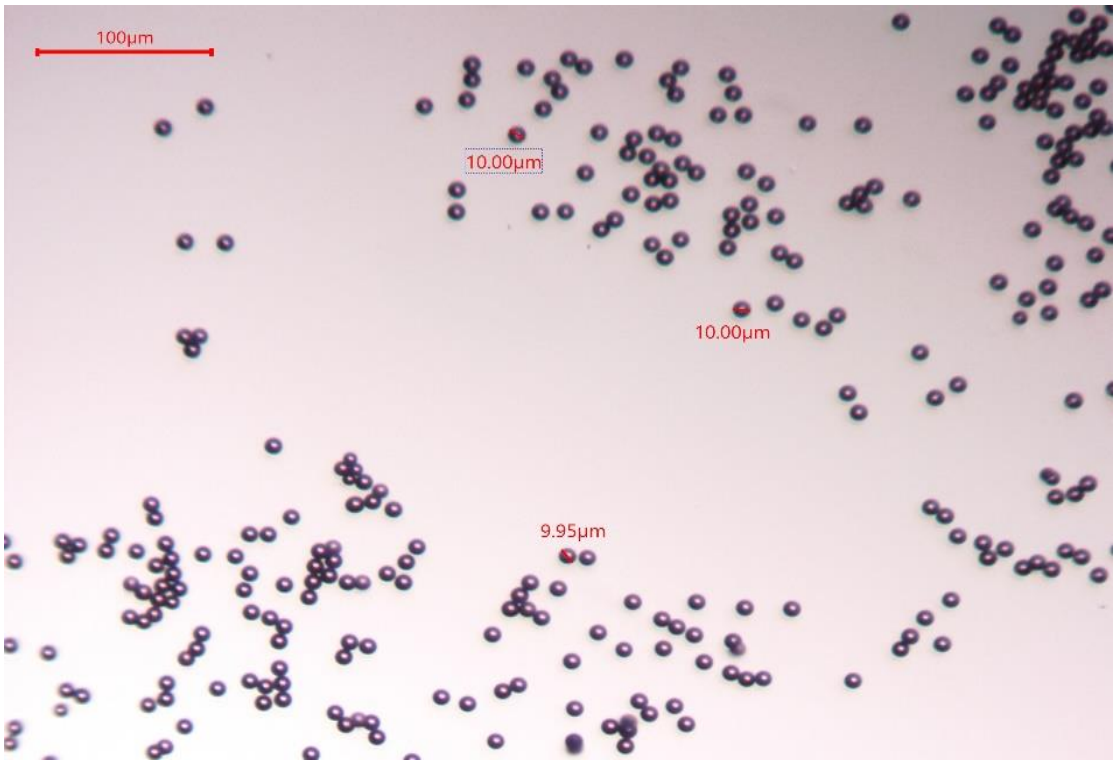

Figure 1.2 Melamine resin with Rhodamine B

CHAPTER 2

THEORY

2.1 Tracers

The tracer is described by American Heritage dictionary as''An identifiable substance which can be radioactive isotope or dye and used in the course of a chemical, mechanical or biological methods [7]. Tracers are used to supply information about feature of the methods and the dispersion of the objects included in it. Generally tracers are categorized in two parts: Conventional and Radioactive tracers.

Radioactive tracers refer to elements constituting radioactive particles to facilitate easier forecasting. Radioactivity is regulated through precipitously transmitting energy as elements by degenerating their nuclear cores. For example, radioactive Tritium (hydrogen-3) molecule produces water particle through balancing the hydrogen atom. The primary difference amongst tracer atom, inclusive of tritium infers that particle sustainability exhales radioactive elements that can be identified through a Geiger counter or other forms of equipment capable of radioactive identification [8].

Radioactive tracers have numerous applications in different fields of science, innovation, farming, medicine and industry. For instance, oil-producing organisations could variate between using standadised pipelines for transportation of crude material from field to refineries. This involves recognizing when the various involved departments and organisations know that the requisite oil is passing through their pipelines. Adding a radioactive tracer to the oil is one approach to fix that issue. The Geiger counter can be utilized to track incoming oil, along with its characteristics. Radioactive tracers are additionally used to decide the area of fractures made by hydraulic fracture in natural gas production.

Conventional tracers are mainly chemical tracers, dyes, surfactants, biological substances and water soluble alcohols [9]. These are the soluble salts as NaCI, $CaCI_2$, as well as potassium or lithium salts or other chemical substances such as borax, boric acid, bromoform, sodium tetraborate, nitrates and dextrose. Rhodamine-B, fluorescein, methylene blue, eosine, fuchsine and ryalux are examples of dyes. Mainly, detergants are used in oil production as surfactants, but because of microbiological decomposition and absorbtivity surfactants are not used too much but they are usable in the observation wells to detect surface tension variations. Also, use of biological substances are limited because biological substances are applicable in purified places, may be of violaceous bacteria, antityphic bacteriophage, E-coli. However, Iyopodium clavatium has given good results in karstic zones. The lower alcohols (methyl, ethyl and isopropyl alcohols) are preferentially soluble, can be transported in water solution and detectable chromatographically. Refractometry, spectrometry and conductimetry are analytic approaches to recognize conventional tracers.

An ideal tracer must have some characteristics:

- Its appearance and even, most often, its amount must be easy to determine even when its concentration in the reservoir fluid domain is too low.

- must be chemically inert

- must not decay or precipitate in the solution arranged for injection in the reservoir.

- must be effectively transported by the fluid

- must be invulnerable to decimations by microorganisms all along its flow direction in reservoir.

- must not be adsorbed, absorbed or trapped by the formation rock

- because of the short time range tracer must be easily injected.

- must be low expense and its use must involve simple, quick and low cost routine techniques

- must not cause dangerous contamination in the reservoir fluid

- Finally, it must be non-poisonous under normal working conditions.

Recent studies about nano- micro technology have focused on creating techniques to describe fracture systems inside a reservoir. The size, shape and connectivity of fractures is critical for characterizing the reserovoir. For understanding fracture distributions, temperature and concentration measurements obtained by nano and micro particle tests can be used.

Various kinds of nano and micro particles involving color connected silica, thermochromic polymer, tin bismuth amalgam and silica embodied DNA particles have been examined [10]. For understanding the temperature dissemination of the reservoir and characterizing the fracture network conclusively, micro-tracers should be transported in reservoir without keeping them in the formation fractures and pores. Thus, mobility of particles was examined in fractured rocks. Particularly, laboratory experimental studies with micro particles were studied.

2.1.1 Tracer Applications in Reservoir Engineering

Tracer applications have improved significantly in different field of studies such as; petroleum engineering, chemical, geothermal engineering and medicine. For example; Vetter and Zinnow give many examples for using tracers in reservoirs [11]. Davis reviewed the usage of tracers in groundwater aquifers [12]. Gaspar and Oncescu demonstrated the properties of common tracers and their analysis methods and applicability in hydrology [13]. Brigham and Deghani gave another example to decide reservoir heterogenities by examining tracer flow [14]. Tracer applications can be found in drilling, well completion, well treatment and enhanced oil recovery.

- *Drilling*: Dangerous situation such as blowout can be foreseen by using tracers, because excessive fluid which move tracers during circulation. Also, the amount of mud filtrate invaded the formation water may be determined. In addition, Edison gave information about using radiotracers to determine circulation losses [15].

- *Well completion*: The location of casing leaks and cement top behind casings can be detected by using radiotracers. In addition, the location of lost circulation wellbore can be obtained by using tracer blended with the slurry [16].

- *Well Treatment*: For understanding fracture characteristics, tracers are blended with proppent agents. Tracers are also used in acidizing for controlling the extent of formation exposed to acid [9].

- *Enhanced Oil Recovery*: One of the important applications of conventional as well as radioactive tracers in oilfield operations is in the secondary and tertiary recovery of oil. Tracers are mostly used in:
  1. Decision of residual oil saturation,
  2. Organize an injection plan for water flooding operation,
  3. Find out the path between injection and production points.

Tracer movement between wells relates information on the movement of traced fluids in the reservoir. Primary information concerns flow rate. Sweep efficiencies and fluid loss into non-producing zones can be determined. If more than one production well is operated flow directions and communication between wells can be tested. Tracers are almost perfect means to quantitivaly determine the flow distribution between flow channels of varying permeability.

Tracer tests may be conducted using a single well, double well or multiple well configuration. In a single well test, tracer is injected in one well and samples are taken at locations near the wellbore. In two well tests, tracer is injected in one well and effluent samples are collected from a production well. This thesis covers a laboratory modification of this type of tracer test. In multiwell tracer tests, a number of tracers are injected and effluent samples are collected at different wells in the field. This type of test was first applied in Loz Azufres geothermal field. Tracer tests are mainly applied ‘‘slug’’ or ‘‘continuous’’ form. Slug form is mostly used because the price paid for continuous injection is higher than slug form. In slug tests, a slug of tracer is injected into the reservoir and then is displaced by reinjected fluid toward the monitoring point or points.

Some properties of tracer samples collected at the production wells are analyzed to detect the phenomena occurred during its travel through the reservoir. Those properties may be amount conductivity, activity or color that are calibrated to give the amount of tracer recovered after the injection. Therefore, some methods of analytical chemistry

such as conductimetry, titrimetry, photometry or colorimetry are helpful in detecting the tracer samples collected.

2.2 Geothermal Systems

Geothermal systems can be depicted as convecting water in the high outside of the Earth crust. Most of the earth's thermal energy is contained within the core and mantle at depths inaccessible to modern exploitation techniques. A reservoir, fluid and a heat source are three fundamental components of geothermal frameworks. (Figure 2.1). Most of these components are found in the vicinity of recent tectonomagnetic activity, such as volcanism and mountain building. The heat source is typically a magmatic intrusion which has rised at shallower depth. The energy within a geothermal reservoir comprises heat stored mainly in rocks, and to a lesser extent, in the fluid that fills the pores and fractures of the rocks. The fluid provides the vehicle for the convective transfer of the heat from deep sources to shallow, drillable levels. Fluid also serves as the means by which geothermal energy escapes to the surface in hot springs and fumaroles and by which this energy can be tapped commercially. The fluid in most geothermal reservoirs is liquid water that is held above surface boiling by the confining subsurface pressure. The withdrawal of liquid water descreases the pressure and causes steam to form, thereby releasing a mixture of steam and water at the surface. Water is the geothermal liquid and this water regularly conveys with chemicals and gases, for example, CO_2 and H_2S. The component hidden geothermal systems is all things considered administered by liquid convection. Convection occurs due to the warming and resulting warm extension of liquids in a gravity field. The Earth's thermal energy is mostly found in the core and mantle, but by using contemporary drilling techniques it is impossible to access this depth. Economic geothermal anomalies are associated with high temperature, porous rock including steam or water. Generally geothermal anomalies are found near environs of tectomagnetic activity and volcanism.

Geothermal reservoir should meet some needs to have an economical potential [17]:

- High temperature,
- A Drillable depth,
- Adequate permeability for heat transfer
- Adequate water to regenerate the system for extended time

There are some types of geothermal reservoirs form on their physical possessions [17]:

1. Vapor dominated convective hydrothermal systems
2. Liquid dominated convective hydrothermal systems
3. Magma systems
4. Geopressured resources
5. Impermeable dry-rock systems
6. Crustal-lift systems

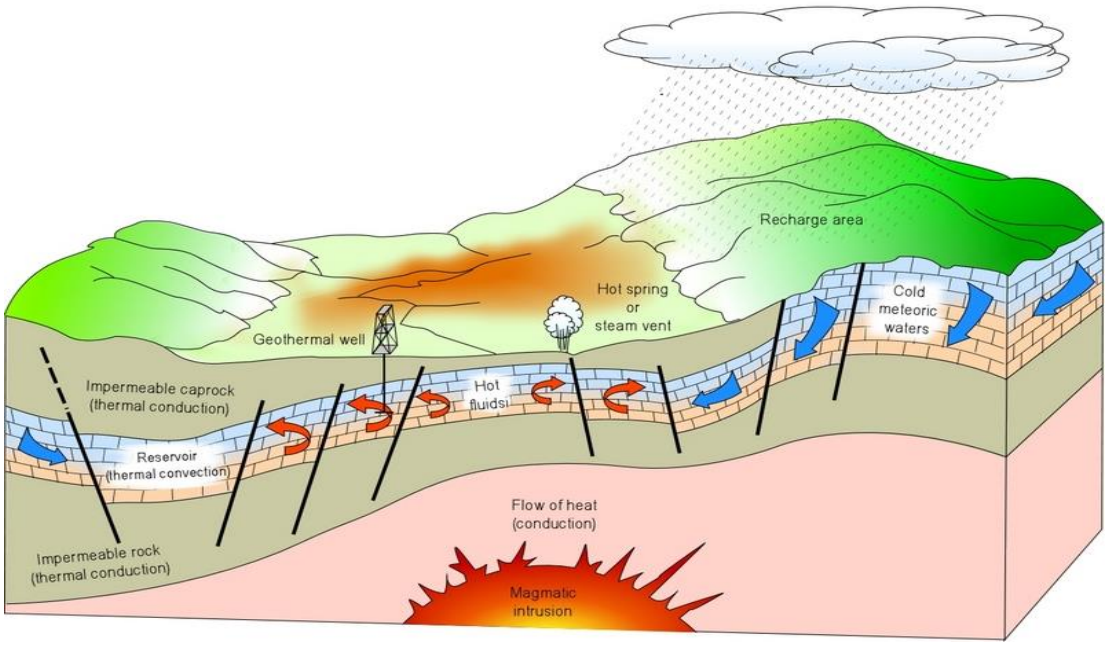

Figure 2.1 An Ideal Geothermal System [18]

Many applications of geothermal energy have been developed in the last years. Generally geothermal energy is used for electricity production, agriculture, house heating and fishery. On the other hand, in the production of geothermal energy different problems may arise: These problems are environmental pollution and scaling through wellbores and pipes.

2.3 Geothermal Reinjection

Geothermal reinjection, which includes injecting energy drained liquid once again into geothermal systems, is a basic piece of all advanced, economical and naturally amicable geothermal use systems (Figure 2.2). It is a productive technique for waste water disposal and in addition, a way to give extra revive to geothermal systems.

Nearly all modern geothermal power plants have constructed and planned to use reinjection to a major range.

Reinjection is accepted as a necassary practice approximately fifty years ago. The first reinjection in high temperature reservoirs occurred in El Salvador [19]. At Larderello in Italy reinjection began in the first half of 1970's as a method for discarding steam condensate [20]. Reinjection is currently a vital piece of the Larderello field operation for enhancing heat recovery.

The aim of using reinjection at the geothermal systems are:

1. Disposal of waste water because such waters frequently contain chemicals harmful to the earth and causing warm contamination [21].

2. Supply extra natural energy to geothermal reservoirs.

3. To enhance thermal extraction from reservoir rocks.

4. Pressure support for balance, decreasing pressure because of mass extraction.

5. To prevent subsidence because of decrased pressure

Although its extensively used in the geothermal systems, reinjection still has some important engineering difficulties. Firstly, the chemicals dissolved in the waste water have a tendency to precipitate in the well and obstruct additional injection. Secondly, returning injection water to production wells can cause decline of the steam flowrate and discharge entalphy. Another difficulty is likelihood of the injected cold water to break the zones adjacent production region hence, effectiveness of the operation can be reduced extremely.

Therefore, for minimizing interference, injection and production wells should be as far as possible and flow-paths need to be completely figured out before reinjection project [22].

Reservoir engineering suggests three useful tools in order to choose a reinjection strategy before conducting it in the fields. Those tools are injectivity testing, well testing and tracer testing.

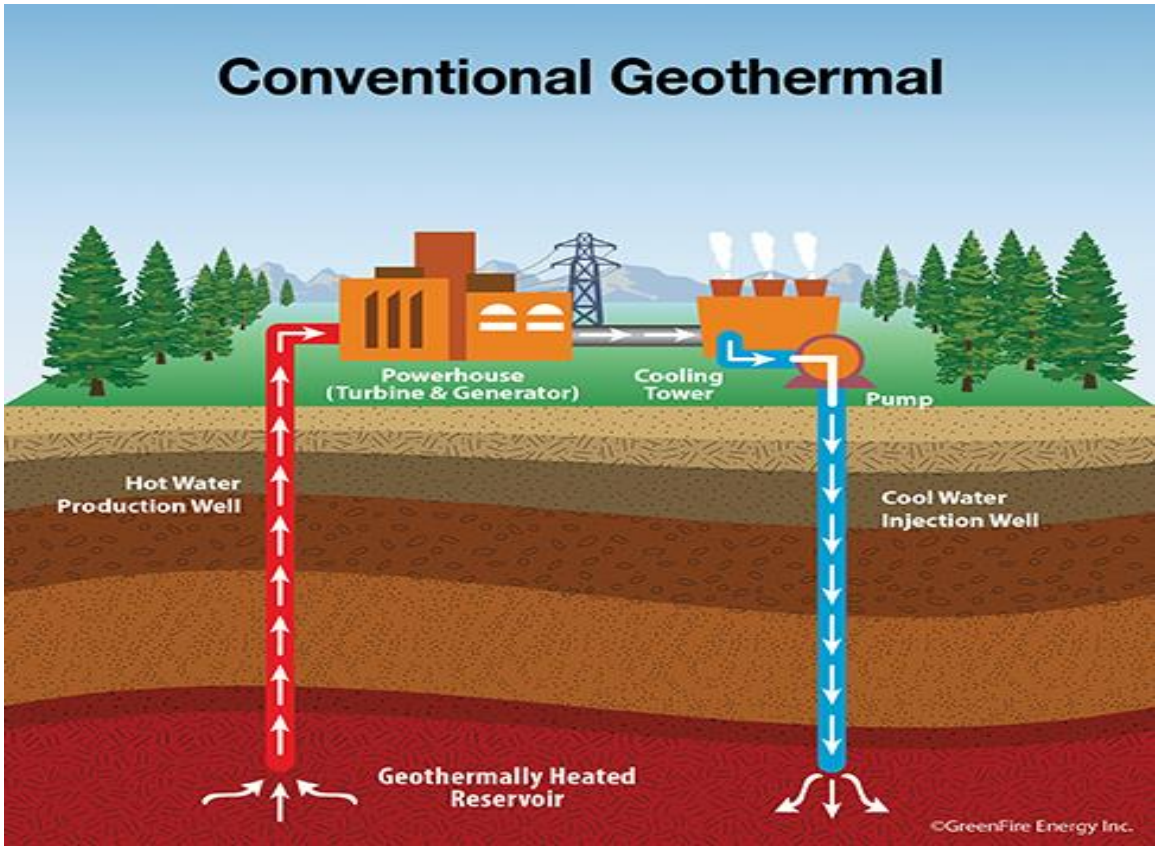

Figure 2.2 Conventional Geothermal Systems [23]

2.4 Tracer Tests in Geothermal Reservoir

Tracer tests give significant data and with these data reservoir engineering can model the path ways of the liquid between from injection wells to production wells. The harmful effects of cool water can be diminished by observing production and injection wells. Tracers are used for both surface and subsurface studies and additionally contamination and atomic waste deposition projects. By adding chemical tracer to the injection systems, the researcher can observe and develop tracer concentration-time curve to understand flow paths between production and injection wells. There are many tracer applications in geothermal history.

For example; McCabe used radioactive tracers to determine flow velocities and directions [24]. Nakamura observed short-circuiting and a decline in production due to cold water entry [25]. Gudmundsson reported a rapid tracer breakthrough in one of the six production wells as a result of sustained injection into one well and also

indicated that iodide seems to be an ideal tracer for high temperature geothermal systems [26].

There are numerous tracer utilizations in geothermal projects [3]:

1. The fundamental reason of using tracer in geothermal application is to understand hydraulic connection of production and injection wells. With the outcomes of tracer tests, researchers can estimate the production wells' cooling times, because of injection colder liquid to reservoir for long times

2. Tracer tests can be applied to Enhanced Geothermal Systems to understand the hydraulic links between production and injection wells.

3. Tracer tests can be conducted for subsurface applications such as understanding underground hydrology and flow.

4. Tracer tests also can be used to estimate the stream ratio of two stages water blended ducts.

These are the most popular tracers utilized as part of geothermal applications:

Liquid-phase tracers:

- Iodide (I) or Bromide (Br)
- Radioactive tracers (^{125}I) and (^{131}I)
- Fluorescent dyes; fluorescein or rhodamine
- Aromatic acids; benzoic acid
- Naphtalene sulfonates

Steam-phase tracers:

- R-134a and R-23
- (SF_6) (Sulphur hexafluoride)

Two-phase tracers

- (^{3}H) (Tritium)
- CH_3OH (metil alcohol), C_2H_6O (Etil alcohol), $CH_3CH_2CH_2OH$ (propanol)

In some different geothermal projects, fluorescein was utilized effectively, because fluorescein can be detected easily even at very low concentrations [21]. On the other hand, utilizing fluoresceın has some drawbacks because it decomposes when the reservoir temperature is above 200°C.

2.5 Micro Tracer Tests in Geothermal Systems

In the development of geothermal systems, the estimation of the size, shape and distribution of fractures is pivotal. Because of its microscopic characterization ability, flow in porous media has huge benefits with an extensive potential for nano-micro technologies. Micro-colloids have been suggested as 'smart' geothermal tracers. These smart tracers give information about flow-path temperature and mapping flow field. Recently, microparticles have been used in applications such as; medicine, colloid chemistry and biochemistry [27]. Also, these microparticles have been used as tracers in environmental science. Especially, fluorescently labeled melamine resin microparticles that are different size and different colour are used. Green fluorescence, Rhodamine B and red fluorescence are typical dyes found in melamine resin fluorescent particles.

Particle transport and maintenance in fractured media differ colossally because of the distinctness in the geometry of transport channels [28]. For finding out the transport mechanisms, examining particle transport in discrete fracture is very valuable and useful. Advection, dispersion, physical straining, adsorption, desorption and air-water interface capturing are mechanisms which effect particle transport in fractured media [29]. A few exploratory examinations of particle transportation in fractured media concentrated on colloid transportation in artificial fractures [30;31;32;33;34], in volcanic rocks [35;36; 37;38] and in fractured clays [39]. Vilks and Bachinski (1996) examined the effect of particle size, velocity and stream way on particle transportation in fractured granite block and inferred that below the critical velocity significant retention of particles was observed due to gravity settlement [38]. In addition, it has been observed that particles transport quicker than moderate solutes in fractured media [36;28;37;40;41]. Due to huge flow paths, fractures are major flow conduits for particles. Bales et al. (1989) investigated the transport of bacteriophages and compared

with conservative solute tracer and concluded that the transport of bacteriophages was three times quicker than moderate solute tracer in fractured porous tuff [35]. McCarthy et al. (2002) investigated the transportation of fluorescent polystyrene particles in fractured shale saprolite and he concluded that the fluorescent polystyrene particles reached much quicker than bromide tracer [32]. Gravitational sedimentation is another important mechanism affecting particle transport in fractured media and it is a function of liquid velocity and by expanding flow rates settled particles might start to move again [29]. Reimus (1995) depicted that gravitational settling, fluid advection and, to lesser degree matrix diffusion, are important in characterizing particle transport in fractures [37].

2.6 Analysis of Tracer Tests

Tracer analysis is a critical strategy for reservoir characterization, especially in geothermal reservoirs. Convection and hydrodynamic dispersion are the two primary processes while the tracer is transported in fractures and porous media. While hydrodynamic dispersion depicts the activities of moleculer dispersion or mechanical blending, convection controls the mass movement of fluids. The flow of tracer has been defined both qualitative and quantitative analysis.

2.6.1 Qualitative Tracer Analysis

Qualitative tracer analysis means interpretation of recovered tracer concentration-time curves. Some siginificant reservoir characteristics such as number of fractures or flow paths and dispersion can be defined by qualitative tracer analysis.

Figure 2.3(a) and (2.3b) can be used for understanding some reservoir characteristics by qualitative tracer analysis. For instance; tracer enters in smaller fractures and dispersion is high in Figure 2.3(a). On the other hand, tracer flows in single fracture and dispersion is low in Figure 2.3(b). Mean arrival times of tracers are shown for each fracture set is given by FAT, SAT and MAT.

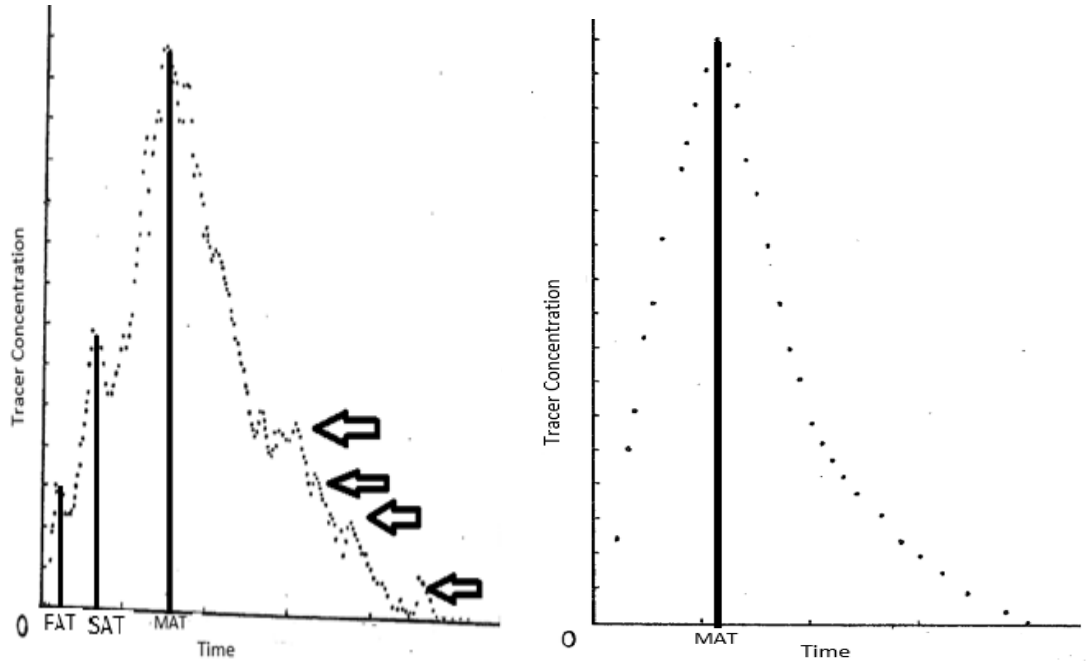

(a) **(b)**

Figure 2.3 Tracer Concentration-Time for (a) and (b)

2.6.2 Quantitative Tracer Analysis

Quantitative tracer analysis is conducted using mathematic models. Tester analyzed tracer returns in a hydraulically fractured geothermal reservoir by using residence time distributions or method of moments to detect interwell flow paths. Satter obtained an analytical solution for chemical transport in porous media [42]. Horne and Rodriguez developed a model considering Taylor dispersion for a tracer flow scheme [22]. Jensen added a retention (matrix diffusion) term to Horne's models to interpret the tracer returns. Jenssen's model used a regression technique to fit the test data with the model data [43]. Sauty produced type curves for tracer tests in 1 and 2 dimensional uniform and radial flow conditions [44]. He also presented analytical models for continuous and slug injection of tracer into the aquifers in one or two dimensional flow conditions.

There are three fracture models; double porosity pseudo-steady-state, double-porosity slabs, double porosity cubes model and three uniform models; uniform porous model, fracture matrix model, and multifracture model in the literature [44;45]. A slug-shaped tracer is injected and effluents are collected from observation wells, and a link between

the production and injection wells is expected. The definition of models are given in the following paragraphs:

2.6.2.1 Multi-fracture model

Fossum and Horne defined a fracture, which connects observation and injection wells. There is high dispersion in this fracture due to high-velocity transport and molecular diffusion.

$$Ct = \sum_{i=1}^{n} e_i \, C_r\left(\frac{R_i}{u_i}, Pe_i\right) \qquad (2.1)$$

C_t : Transfer function,

n : Number of flow channels in the fracture system,

e_i : Flow contribution coefficient,

R_i : Apparent fracture length, (cm)

u_i : Velocity, (cm/s)

Pe_i : Peclet number of i^{th} flow channel

It is necessary for single and multi systems to feature a minimum of 2 fractures, Transfer function, C_t, has no correlation with increasing volume of n [46], thus a model with 3 fractures represent multifracture systems successfully.

The C_r can be defined for all paths of tracer mass released on x=0 at time=0 as,

$$C_r = J\frac{1}{\sqrt{t}}\frac{2t_m}{t}\exp\left(\frac{-Pe(t-t_m)^2}{4t_m t}\right) \qquad (2.2)$$

Pe infers a Peclet number that defines advective transport rate divided by diffusive transport rate and flow contribution coefficient (e_i) is defined as contribution effect of flow in i_{th} channels in multi fracture systems.

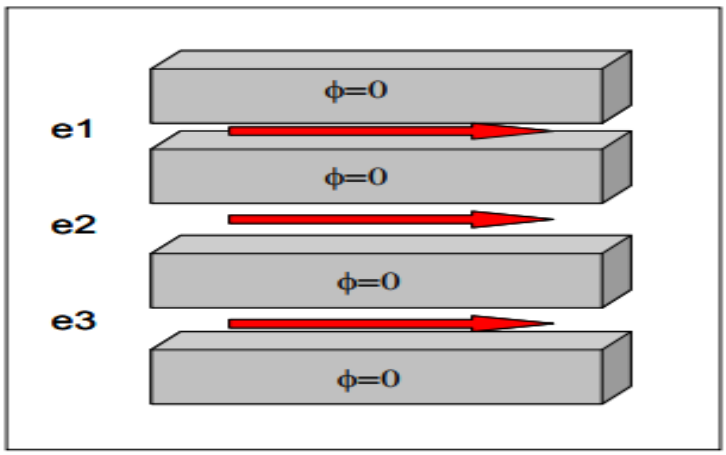

Figure 2.5 Multi Fracture Model Design[47]

t_m refers to the average tracer arrival time measured in seconds, whereas J is a parameter obtained from the folowing equation:

$$J = \left(\frac{m}{4Q}\right)\left(\frac{Pe}{\pi t_m}\right)^{\frac{1}{2}} \quad (2.3)$$

Using multi fracture model and knowing the Q, which refers to volume production rate, R, which infers the measure distance between the producer and injector, it is possible to obtain m, mass of tracer and the dispersion coefficient (m^2s^{-1}) for all channels through implementing the following equation:

$$D_{tr} = \frac{R^2}{Pe\ t_m} \quad (2.4)$$

2.6.2.2 Fracture-Matrix Model

In this model, there is a large fracture with micro fractures in the rock matrix on either side according to the report of Bullivant and O'Sullivan (1989)[48]. Tracer particles leave from the main fracture and move into the micro facture system. The tracer chemical stay for a while, and then return to the main fracture.

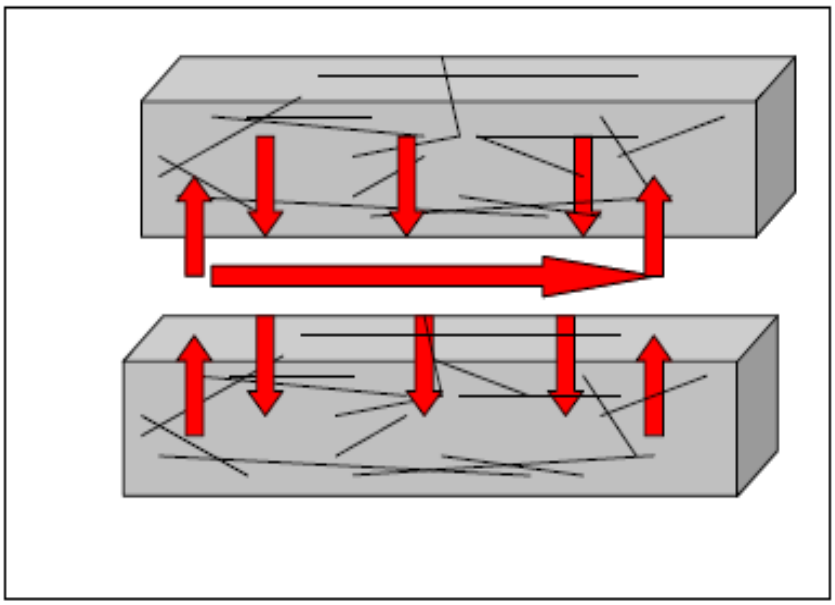

Figure 2.6 Fracture Matrix Model Design [47]

Longitudinal dispersion due to the velocity profile across the fracture is ignored in order to give a clear distinction from the single fracture model. A fracture with fluid velocity constant across the thickness and with diffusion perpendicular to the fracture into an infinite porous medium is used in this model. The solution is in the following form:

$$C_r = JU(t - t_b)^{\frac{-1}{2}} \text{Exp}\ \frac{-t_b}{w(t-t_b)} \qquad (2.5)$$

Where

U = Heaviside step distribution, t_b = the response start time, J is a model parameter

w = A ratio of transport along the fracture to transport out of the fracture

2.6.2.3 Uniform Porous Model

In the uniform porous model, it is assumed that a tracer slug is instantaneously injected into the system, with constant thickness. Similarly, it is also assumed that, the flow is rapid allowing the kinematic dispersion components to be predominant. Sauty (1980) reported for purely hydrodispersive transfer the solution for one 1D flow is,

$$C_r = \frac{K}{\sqrt{t_r}} \mathrm{Exp}\left(-\frac{Pe}{4t_r}(1-t_r)^2\right) \quad (2.6)$$

Where,

$$K = \sqrt{t_{rm}}\, \mathrm{Exp}\left(\frac{Pe}{4t_{rm}}(1-t_{rm})^2\right) \quad (2.7)$$

$$t_{rm} = \sqrt{1+Pe^{-2}} - Pe^{-1} \quad (2.8)$$

Pe = The dimensionless Peclet number,

K = Model parameter

t_r = The mean arrival time,

Similarly, Sauty (1980) also reported an analytical expression for the slug injection of a tracer solution into a 2D field [44].

The solution on the flow axis can be obtained similar to the 1D form as shown below.

$$C_r = \frac{K}{t_r}\, \mathrm{Exp}\left(-\frac{Pe}{4t_r}(1-t_r)^2\right) \quad (2.9)$$

Where,

$$K = t_{rm} \mathrm{Exp}\left(\frac{Pe}{4t_{rm}}(1-t_{rm})^2\right) \quad (2.10)$$

$$t_{rm} = \sqrt{1+4Pe^{-2}} - 2Pe^{-1} \quad (2.11)$$

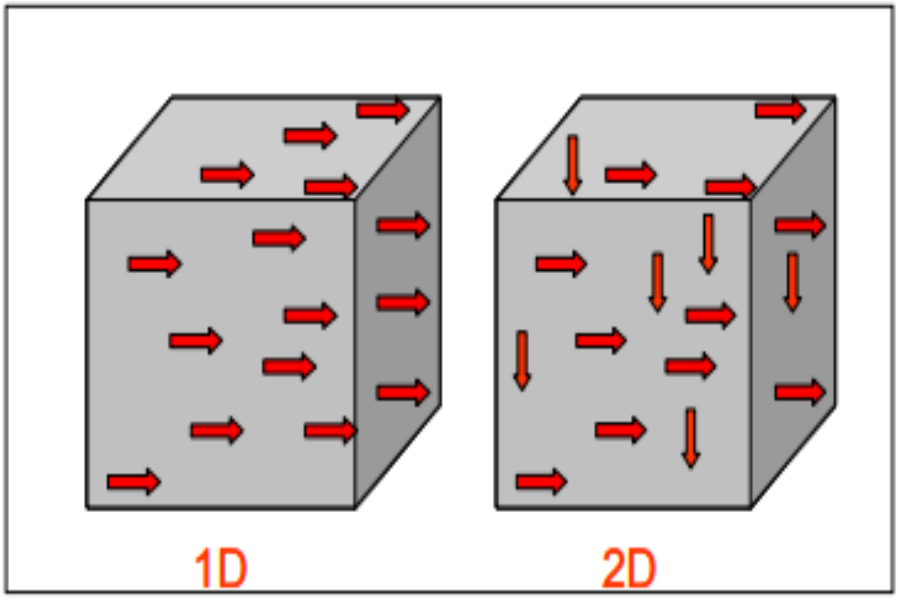

Figure 2.7 Uniform porous model Design[47]

2.6.2.4 Double Porosity Slabs Model

Bullivant and O'Sullivan defines the double-porosity slabs model as parallel fractures with consistent thickness a, separated by slabs of the rock matrix giving a constant seperation b [48] (Figure 2.8).

Tracer movement in slabs is modeled by diffusion perpendicular to the fractures. If the response start time, t_b, matrix block fill up time, t_f, the ratio of transport along the fracture to transport out of the fracture, w, and the model parameter, J, and the injection rate, Q are known, p laplace inversion parameters, the mass of tracer, m, and the ratio of fracture porosity ϕf to matrix porosity ϕm can be estimated by using the following equation.

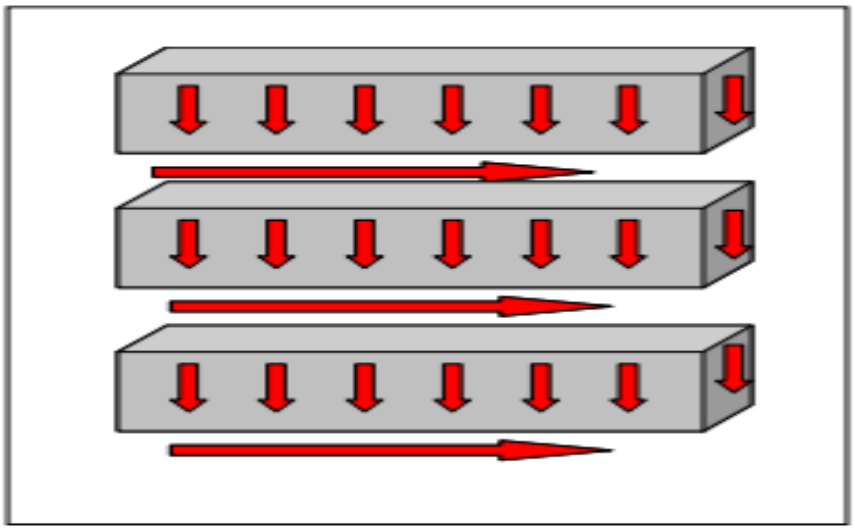

Figure 2.8 Double Porosity Slab Model Design [47]

The solution is given by the following equation: Here p is the laplace transform parameter.

$$C_r = JExp(-t_b\left(2\sqrt{\frac{p}{wt_b}}\tanh\left(\frac{t_f}{2}\sqrt{\frac{p}{wt_b}}+p\right)\right)) \quad (2.12)$$

2.6.2.5 Double Porosity Cubes Model

Bullivant and O'Sullivan defined the double-porosity cubes model as the rock matrix consists of cubic blocks of side b seperated by high permeability fractures of aperture "a". (Figure 2.9).

The double-porosity cubes model differs from the double porosity slabs model because for the cubes model, the area of the surface a distance b/2+z from the nearest fracture is proportional to the square of z, whereas for the slabs model the area of the surface a distance b/2-z from the nearest fracture does not differ with z. This affects the way tracer diffuses into the block.

.

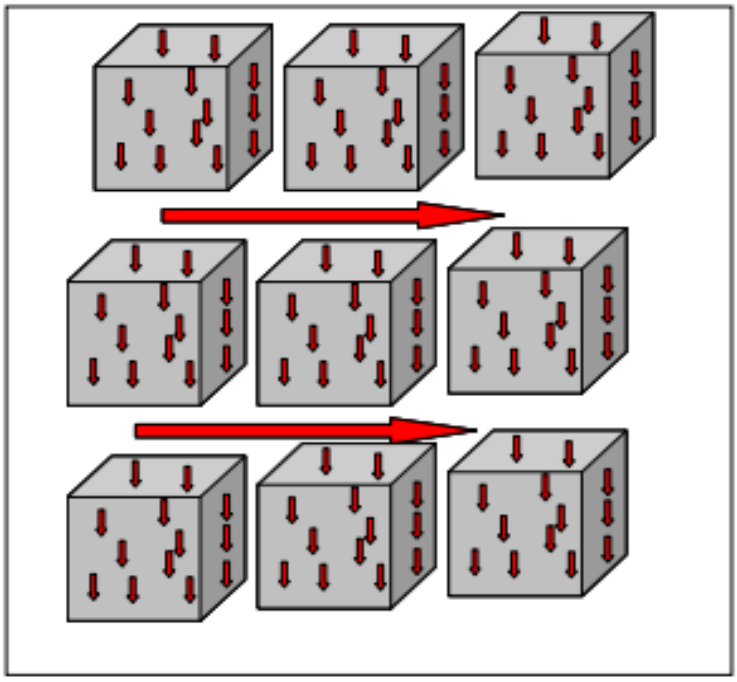

Figure 2.9 Double Porosity Cubes Model Design [47]

The solution is given by the following equation:

$$C_r = JExp\left(-t_b\left(2\sqrt{\frac{p}{wt_b}}\coth\left(\frac{t_f}{2}\sqrt{\frac{p}{wt_b}}\right)-\frac{4}{t_f}+p\right)\right) \quad (2.13)$$

2.6.2.6 Double Porosity Pseudo Steady State Model

For this model, the reservoir contains uniformly distributed high permeability micro fractures which divide the reservoir into low permeability blocks that consist of unswept pores by the fluid flow (Figure 2.10).

Similar to the mechanism defined for the fracture matrix model, the tracer leaves the micro fractures and then returns again. However the effect is different, such that the blocks may be filled with tracer.

Longitudinal dispersion because of the movement of fluid into the micro fracture network is neglected. O'Sullivan and Bullivant (1989) reported the solution for this case and given below. In this equation, α_m means matrix porosity, and α_f means fracture velocity.

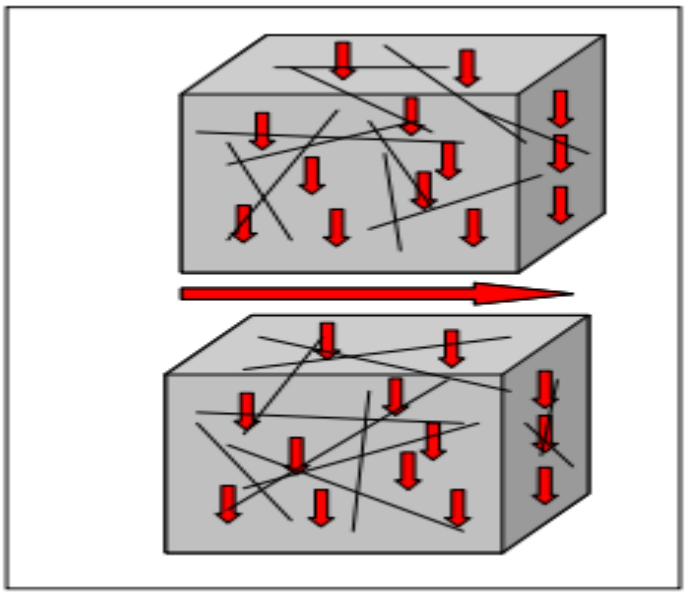

Figure 2.10 Double Porosity Pseudo State Model Design [47]

$$C_r = JExp(-\alpha_m t)U(t - t_b)^{\frac{1}{2}} I_1(2(t_b \alpha_f \alpha_m (t - t_b))^{\frac{1}{2}} \quad (2.14)$$

U is Heaviside step distribution, J is a model parameter, t_b is the time at which the tracer pulse would reach the observation well if there was no dispersion, α_f means the rate of tracer interchange per unit fracture volume and α_m means the rate of tracer interchange per unit matrix volume.

2.7 Tracer Interpretation Using Temporal Moments

The importance of tracer testing is appreciated by more than one hundred geothermal tests conducted worldwide over the latest half century. Tracer test have been used by researchers to constrain numerical models and using the data to estimate heat transfer parameters [19;21]. However, the vast majority of these tests were interpreted qualitatively, ignoring the temporal evolution of the tracer breakthrough curve and resulting in gross test interpretation. This study discusses about methods for extracting useful, quantitative data from tracer testing.

A large group of tracer test analysis techniques consider the temporal behaviour of tracers and these techniques were developed for closed reactor vessels, but have been

applied to more general conditions of open boundaries, characterization of fractured media under continous tracer reinjection [19], and evaluate flow geometry. These techniques have a rigorous numerical basis and offer additional information about the underground.

Tracer tests give significant informations and one can obtain first temporal moment and mean residence time by using tracer test data. The total pore volume swept by a tracer can also be determined from its mean residence [49].

The steps required for accurate tracer analysis are summarized as follows:

- Correct the tracer recovery for thermal decay
- Normalize the tracer history
- Deconvolve the output signal
- Extrapolate history to late time
- Calculation of mean residence time and swept volume
- Calculate flow geometry

2.7.1 Correcting the Tracer Recovery for Thermal Decay

Arrhenius equation is used for correcting the tracer history for thermal decay [49]. For the most part the underground temperature is not known precisely, so appropriate correction is difficult. Some studies have considered this problem and remains a focus of the Idaho National Laboratory Geothermal Technologies Program [19].

2.7.2 Normalizing the Concentration History

The method of moments is based on age distrubition. The age distribution function is referred to E(t) and has units of (1/t). E(t) can be obtained by following equations. C(t) means tracer concentration and ρ is used for calculation of mass fraction.

$$E(t) = \frac{C(t)q_{inj}}{M_{inj}} \quad \text{for C in volume fraction}$$

$$E(t) = \frac{C(t)\rho q_{inj}}{M_{inj}} \quad \text{for mass fraction} \qquad (2.15)$$

Instead of C(t) using E(t) has some advantages because tracer is reinjected, so the output signal is a combined response to the original pulse injection plus recirculation. Moment analysis is based on analysis of a pulse injection, so initially, the impact of recirculation must be removed from the output signal. Deconvolving tracer history is need for changing C(t) to E(t). The area under the curve E(t) versus t is unity in a closed system (100% tracer recovery).

2.7.3 Deconvolving the Tracer History

When tracer is reinjected, the tracer history is a combined response to the initial slug tracer injection and continuous recycling of the produced tracer. Moment analysis is based on response to slug tracer injection, therefore firstly, the effect of tracer recycling must be removed then swept volumes and residence times must be calculated. For deconvolving the tracer response, the convolution integral is used [48]:

$$E_{app}(t) = \int_0^t E_{in}(t-\tau)E(\tau)d\tau \qquad (2.16)$$

Equation (2.16) indicates that, Eapp(t) is the function of Ein and residence time distribution and the derivation of equation (2.15) is presented as follows.

$$E_{app}(t) = \frac{C(t)\rho q_{inj}}{M_{inj}} \qquad (2.17a)$$

$$E_{in} = \delta(t) + \frac{1}{1-f_{loss}} \frac{C(t)\rho q_{inj}}{M_{inj}} \qquad (2.17b)$$

Substituting Equation (2.17b) in Equation (2.15) gives

$$E_{app}(t) = \int_0^t (\delta(t) + \frac{1}{1-f_{loss}} \frac{C(t-\tau)\rho q_{inj}}{M_{inj}})E(\tau)d\tau \qquad (2.18)$$

Reaarranging equation (2.18) gives the correction needed to remove the effects of reinjection:

$$E(t) = E_{app}(t) - \frac{1}{1-f_{loss}} \int_0^t E_{in}(t-\tau)E(\tau)d\tau \qquad (2.19)$$

At each time the integral in Equation (2.19) must be calculated again, using the , C(t) C(t- τ), E(τ). At the upper limit of integration, the argument is zero, so the E(t), current residence age can be calculated at each time step. In summary, if tracer is recycled, or in another words if the tracer injection time isn't small relative to the residence time (ts « t*), the appearent residence time distribution require correction.

2.7.4 Extrapolating the History to Long Time

Regularly tracer samples are finished before tracer concentration becomes zero. The following equation can be used for calculating pore volume estimates and mean residence time for late time.

$$t^* = \frac{\int_0^\infty E(t)tdt}{\int_0^\infty E(t)dt} = \frac{\int_0^{t_b} E(t)tdt + \int_{t_b}^\infty E(t)tdt}{\int_0^{t_b} E(t)dt + \int_{t_b}^\infty E(t)dt} \tag{2.20}$$

If the decline is exponential, the data of tracer can be written as;

$$E(t) = be^{-at} \quad \text{for } t > t_b \tag{2.21}$$

Exponential decline is the most common recognized tracer decline observed, because permeability much of the time appproximates to a log-normal distrubition. Three differing curves are used for calculating late time in tracer test examinations. These curves are linear, power law and exponential.

$$\int_{t_b}^{\infty} E(t)tdt = \frac{b}{a^2} e^{-at_b}(1 + at_b) \tag{2.22}$$

And

$$\int_{t_b}^{\infty} E(t)dt = \frac{b}{a}\, e^{-at_b} \qquad (2.23)$$

2.7.5 Calculating Mean Residence Times

The mean residence time is obtained from the normalized, deconvolved and extrapolated tracer history. The mean residence time is calculated by the following equation:

$$t^* = \frac{\int_0^{t_b} E(t)tdt + \frac{b}{a^2} e^{-at_b}(1 + at_b)}{\int_0^{t_b} E(t)dt + \frac{b}{a} e^{-at_b}} \qquad (2.24)$$

2.7.6 Determining Pore Volume

(Levenspiel 1972) indicated that pore volume is obtained from mean residence time. As following equation (2.25) is used for calculating pore volume [49];

$$V_p = \frac{m}{M_{inj}} q_{inj} t^* \qquad (2.25)$$

2.7.7 Calculating Flow Geometry

Tracer tests give important information about the pore volume (flow and storage) geometry. Streamlines or individual flow paths have unique amount of porosity, permeability, length and cross sectional area.

(Φ) means storage capacity (volume swept) and (F) means flow capacity (amount produced) is the tracer recovery at time=t normalized by the complete recovery.

$$\Phi(t) = \frac{\frac{\int_0^t E(\tau)\tau d\tau}{\int_0^\infty E(\tau)d\tau}}{\frac{\int_0^\infty E(t)tdt}{\int_0^\infty E(\tau)d\tau}} = \frac{\int_0^t E(\tau)\tau d\tau}{\int_0^{\infty\infty} E(\tau)\tau d\tau} \quad (2.26)$$

And

$$F(t) = \frac{\int_0^t E(\tau)d\tau}{\int_0^\infty E(t)dt} \quad (2.27)$$

Flow and storage capacity are most often plotted on F-Φ plot. The shape of the F-Φ curve gives lots of information, for example, it gives the information about the effect of pore volume to the effect of fluid flow [50] and also the slope of F-Φ gives interstitital fluid velocity.

2.7.8 Estimating Heterogeneity

There are two general measures of heterogeneity and these coefficients could be decided by the F- Φ plot. These coefficcients are Lorentz and Dykstra-Parsons coefficient,

The Lorentz coefficient could be calculated by following equation;

$$L_C = 2\left(\int_0^1 F d\Phi - \frac{1}{2}\right) \quad (2.28)$$

The values of L_c varies between 0 and 1. Zero means a homogeneous flow field. Generally, increasing value of L_c means increasing heterogeneity of the flow field.

The Dykstra-Parsons coefficient could be calculated by using the F- Φ scheme.

$$V_{DP} = \frac{F'|_{\Phi=0.5} - F'|_{\Phi=0.841}}{F'|_{\Phi=0.5}} \quad (2.29)$$

2.7.9 Volumetric Fluid Sweep Efficiency

Volumetric fluid sweep efficiency (Ev), could be described as the ratio of volume of reservoir contacted by injected fluid to the total pore volume of the reservoir. Sweep effciency can be defined as (volume of fluid injected) * (1 – part of streamlines broken through). Sweep efficiency is a function of dimensionless units.

$$E_V(t + \Delta t) = E_V(t) + \frac{q_{inj}}{V_p} \frac{m}{M_{inj}} \Delta t[1 - F(t + \Delta t] \tag{2.30}$$

Sweep efficiency is normalized by the total pore volume:

$$t_D = \frac{q_{inj}}{V_p} \frac{m}{M_{inj}} t = \frac{t}{t^*} \tag{2.31}$$

Sweep efficiency is generally plotted E_V versus t_D.

CHAPTER 3

STATEMENT OF THE PROBLEM

Reinjection is an indispensable part of all geothermal field management. Some field parameters related to transport phenomena and transporting medium must be known to develop a reinjection program in geothermal fields. Interpretation procedures for field tracer tests in advance are applied where fracture geometry or flow pattern cannot be known. Conventional tracers that dissolve in water have been used widely and successfully in geothermal fields for understanding fracture connectivity because of their economical nature, stability at reservoir conditions and ease of detection at extremely low concentrations. Although conventional tracers can provide a wide range of information about flow paths such as dispersivity, fluid velocity, Peclet number etc. with developed flow models, they are still insufficient for detailed evaluation of transport system of the fractured rock. Therefore, nanoparticle and micro particles have been introduced to overcome the restrictions with conventional tracers in fractured rocks.

The purpose of this study is to to investigate the applicability of the micro melamine resin as a tracer in geothermal reservoirs. Conventional Rhodamine B and micro melamine particles were compared. In addition, the effect of particle size, injection rate and fracture geometry on the recovery and retention of micro particles also investigated to identify connections of fractures in a low enthalpy experimental geothermal reservoir model.

CHAPTER 4

EXPERIMENTAL SET UP AND PROCEDURE

Because of the high cost of micro tracers and conventional tracers, ‘‘Slug type’’ injection was planned. Rhodamine B was selected as a conventional tracer and micro particles based on melamine resin Rhodamine B marked was selected as micro tracer in this study. Rhodamine B was selected due to its easy measurement property therefore, generally it is utilized in low enthalpy geothermal applications.

A low temperature geothermal reservoir model was built from 25 marble blocks with block dimensions of 5x10x10 cm (Figure 4.1). Another system was built with the same concept but 50 marble blocks were used with block dimensions of 5x5x10 cm (Figure 4.2). Two different models were designed to understand the effect of different facture densities on tracer concentration-time curves and temperature distributions. The models were designed in such a way that the tracer was injected as a slug from the left bottom corner of the reservoir and samples were collected from the upper right corner of the system in 1 minute time intervals. Both conventional tracers and micro particles with different sizes (4 μm, 6 μm, 10 μm) melamine resin Rhodamine B marked tracers were used in both models and results were compared. In addition, the effect of different injection flow rates (15 ml/min, 30 ml/min, 45 ml/min) on tracer recovery for both conventional tracers and micro tracers were investigated and compared. The models represent a low enthalpy geothermal reservoir that produce from shallow depth and injection into the deeper zone. Distilled water (20°C-25°C) was used as the reinjected fluid and before each run, the model was recharged with distilled water. Injection and production rates were kept equal, while continuous water injection, temperature and pressure were recorded in the several parts of the system.

4.1 Set-up

Two reservoir models were built from marble blocks. There are 25 marble blocks with dimensions of 5x10x10 cm and 50 marble blocks with block dimensions of 5x5x10 cm. In this study, setting up experiments took about nearly 5 months because of some problems such as leakages, late supplying micro particles, repairs and calibration of thermocouples and scanner.

4.1.1 Two Dimensional Fractured Model

In the first model, 25 marble blocks with dimensions of 5x10x10 cm blocks were used to create a fractured medium (Figure 4.1). In the second model, 50 marble blocks with block dimensions of 5x5x10 cm blocks were used to create a fractured medium (Figure 4.2).

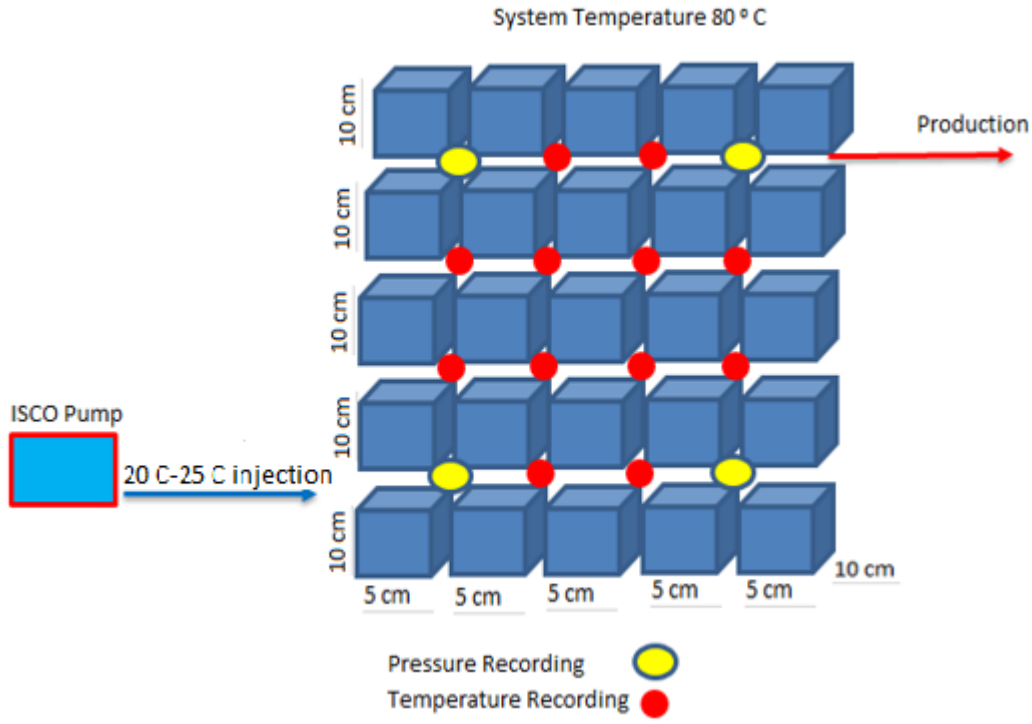

Figure 4.1 Model-1 which consists from 5x10x10 cm dimensions of marble

An ST- 138 steel box frame of 50 x 25,7 x 10,7 cm in dimensions were utilized to cover the fractured medium. Four corners of the model were welded to each other with lower plate. Then, 0,8 cm diameter steel bolts and nuts were utilized to connect the upper steel plate to connect to the model. In addition, çekomastik liquid gasket was used for prevent the leakages and to fill the void space between the walls of steel box and those of marble blocks in order to avoid the effects of boundaries on the experimental conditions. The models were installed in an oven in order to maintain the temperature at a constant volume.

After the blocks were packed, the system was filled with distilled water for determining the porosity of the system. The total volume of the system was 13750 cc and a 1450 cc-pore volume of the system created 10,53% porosity for the first model and 1300 cc-pore volume of the system created 9,38% porosity for the second model.

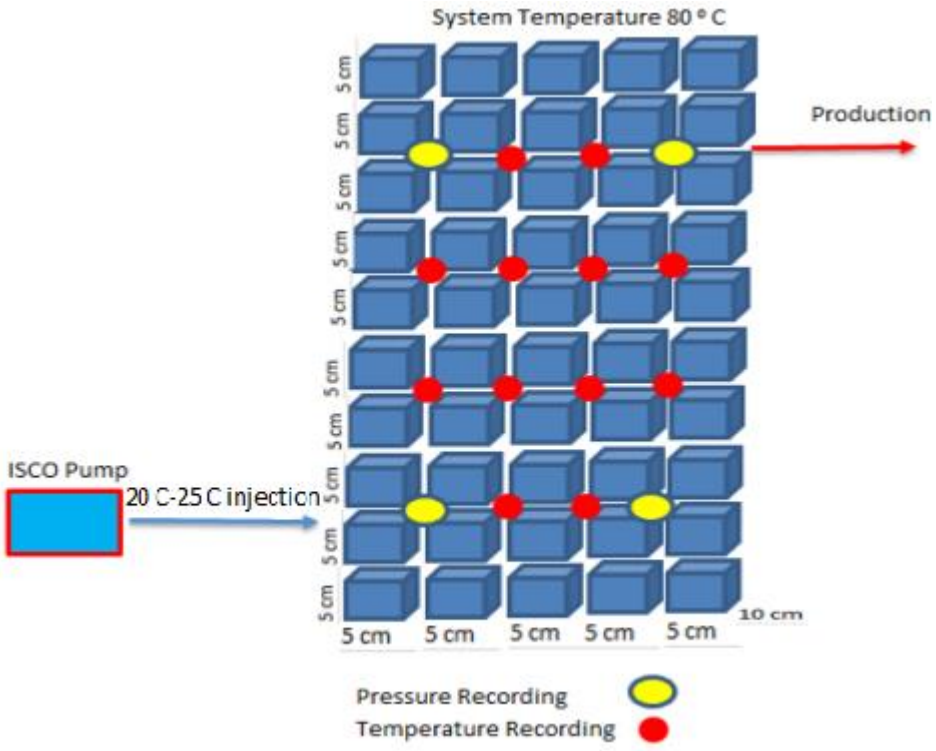

Figure 4.2. Model-2 which consists from 5x5x10 cm dimensions of marble

Figure 4.3. Model-1 and Model-2 marble blocks

4.1.2 Thermocouples

12 thermocouples 3xFe-const. types are used in experiments. All of these thermocouples were connected to a temperature scanner. Thermocouples are produced by Elimko Ltd. Half of them was installed on the top and the other half was installed at the bottom section of model, symmetrically. First and third layers were at 10 and 30 cm from the bottom, respectively and second and four layers at 20 and 40 cm from the bottom, respectively.

4.1.3 Scanner

An AB-100 type, 60 channel scanner made by Elimko Ltd. was used to track thermal changes within the system. The milivolt values come from the thermocouples by means of a calibration wire were transmitted to the digital thermometer and displayed as degrees centigrade.

4.1.4 Pressure Transducer

Pressure transducers (Gem) were used to collect the pressure data at the corner of the models. The measurable pressure range between 0-7 barg and 4-20 mA.

Figure 4.4 Thermocouples, Pressure Transducer and Scanner

4.1.5 260D Syringe Pump

The 260D Syringe Pump which is the first Isco D-Series pump module was used in this experiment. This pump supplies pressures up to 517 bar and a flow rate ranging from microliter to 107 mL/min. In this study, this pump is used to provide different injection rates.

4.1.6 The Turner Quantech Digital Filter Fluorometer

The Turner Quantech Digital Filter Fluorometer is intended to perform scientific quantitative fluorescence estimations on different fluorescent materials including fluorescein, histamine, rhodamine, vitamins, chlorophyll, DNA/RNA dye complexes and other fluorescent compounds. In this study, FM109510-33 Base Model Turner Quantech Digital Filter Fluorometer which has wavelength range 340 - 650 nm was used to measure concentrations of unknown effluent samples.

Figure 4.5. 260D Syringe Pump and The Turner Quantech Digital Filter Fluorometer

4.1.7 Micro Particles Based on Melamine Resin, Rhodamine B-Marked

Micro particles based on melamine resin, rhodamine B-marked, products were purchased from Sigma-Aldrich. Melamine resin microspheres are made by corrosive catalyzed aqueous polycondensation of methylol melamine in the temperature scope of 70°C to 100°C with no surfactants. Sigma Aldrich Inc. states that density of microsphere particles is 1.51 g/cm^3, the particles are stable at temperature up to 300°C and they are stable in acids and bases. Surface of the particles is hydrophilic. Melamine resin fragments' sizes and shapes were scanned by utilizing a polarizing transmitted light microscope. The particles are labelled with fluorescent dye of red color (Figure 4.6).

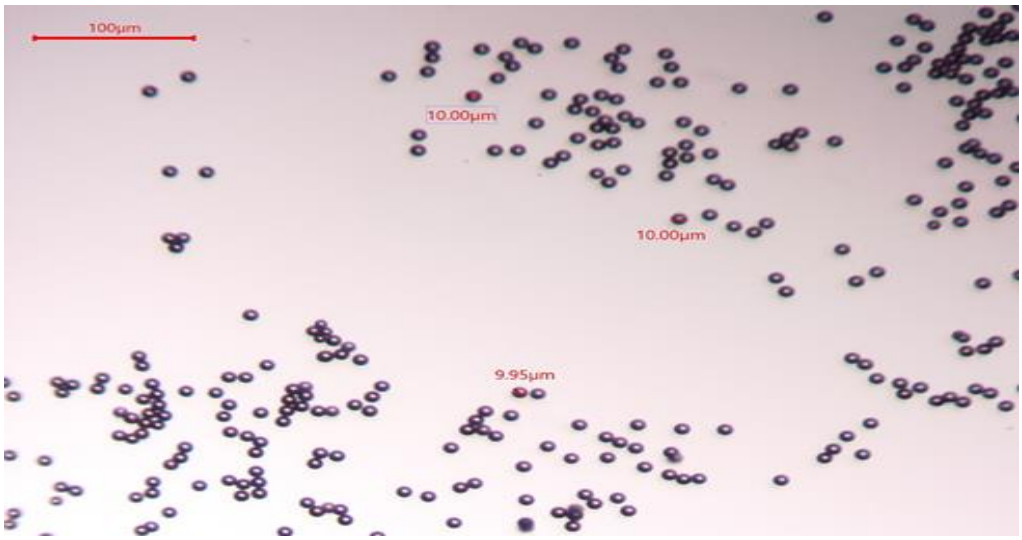

Figure 4.6 Micro Particles Based on Melamine Resin, Rhodamine B-Marked

4.1.8 Transmitted Light Microscopy

Nikon Transmitted Light Microscopy was used for scanning particles and Figure 4.6 was taken by transmitted light microscopy for observing melamine resin particles.

Figure 4.7 Transmitted Light Microscopy

4.2 Procedure

The first criteria for this experiment is thermal eqilibrium in the model. The system was heated up to 80^{o}C for all experiment runs and this took 8-10 hours. The temperature in the model was monitored by scanning 12 thermocouples present in the system during heating the system.

When the system reached desired temperature of 80^{o}C, the experiment was started. The tracer was injected as a slug form from the left bottom corner of the reservoir at between (20 ^{o}C -25 ^{o}C) and samples were collected from the upper right corner of the system in 1 minute time intervals. After the injection of tracer or micro tracer slug, distilled water was used to displace the slug of tracer in the system. This continued until little or no tracer/micro tracer was observed in the effluent.

After each run, effluent samples were collected and the Turner Quantech Digital Filter Fluorometer was used to measure concentration values of experimental runs. The calibration run of the fluorimeter was conducted at different concentrations (i.e 0.25, 0.5, 1.0, 5.0, 75, 150 ppb). If the regression constant of the calibration line was bigger than 0.95, the concentration of effluent samples can be measured correctly and at the beginning of each experiment the calibration of the fluorometer was conducted. Then, the system was prepared for the next experiment.

CHAPTER 5

ANALYSIS OF DATA

The breakthrough curves which were collected as the effluent concentration of the tracer was the most significant result of the experiments. By examining experimental data, porous medium parameters (Peclet number, fracture length, porosity etc.) and transport parameters (velocity, mean arrival time, first arrival time etc.) can be identified.

The process for calculations is to match the experimental breakthrough curve with that of the model by using least squares approximation. Once a good match was obtained, reservoir model parameters were then determined by using corresponding equations. By minimizing the sum of the square differences, multi-fracture model was best matched with our tracer experiment data. The Generalized Reduced Gradient (GRG2) nonlinear optimization code was used in Microsoft Excel Solver.

$$R = \sum_{i=1}^{n} w_i \left(C_{model} - C_{experiment}\right)^2 \qquad (5.1)$$

Here w_i's are the inverses of the variances of the experimental measurement errors, which will give the maximum-likelihood/minimum-variance estimates of the parameters [50]. The parameters of the proposed analytical transfer functions can be assessed with minimizing the target cell, R. It is important to starting with good initial estimates in nonlinear parameter estimation or curve fitting. However, initial estimates of Peclet numbers should be done by experimentation (trial-and-error) method. The peak time could be found from test data. The methodology can be summarized as follows. Initially, the target cell (R), changing cells (Pe, etc.), and the constraints (Pe>0, etc) are determined. Then, the solution time, the number of iterations and the precision of constraints that control the solution process are defined.

Then the method used by 'Solver' is characterized. At this point (tangent or quadratic) which is assesment approach, (Central-forward difference equation) the technique for calculating derivatives, and lastly the search technique (quasi-Newton or conjugate) must be defined. Then solver achieves a solution to determine the accuracy of the estimation. 95% confidence intervals were used for assessing of tests and an acceptable estimate was defined that the one with a confidence interval which is no less than 10% of the value. If one of the changing parameters exceeds 10%, initial estimates of the of changing criteria were rearranged and calculations were repeated until the point when reasonable values was accomplished. The parameters and calculation values of 10 μm 15 cc/min are given in Table 5.1. Parameters and calculation values of conventional rhodamine B with 5 cc/min, 15 cc/min and 4 μm with 15 cc/min, 6 μm with 15 cc/min are given in Appendices part of the thesis.

Table 5.1: Parameters and Calculation values of 10 μm, 15 cc/min in 5x10x10 cm

5x10x10, 210 ppb, 10 μm, 15cc/min					
Fracture-I		**Fracture-II**		**Fracture-III**	
mean arrival time (min)	117	mean arrival time (min)	50	mean arrival time (min)	13
Pe	4,7	Pe	2,9	Pe	1,5
J	1,494	J	14105	J	0,987
e1	0,574	e2	7E-05	e3	0,423
et	0,998				
Lenght,cm	37,5				
Injection rate,ml/min	15				

Calculations					
mean velocity (cm/min)	**0,32**	**mean velocity (cm/min)**	**0,75**	**mean velocity (cm/min)**	**2,99**
Disp. coeff. (cm^2/min)	2,6	Dispersion coeff. (cm^2/min)	9,8	Dispersion coeff. (cm^2/min)	72,5
tracer mass (ug)	0,796	tracer mass (ug)	6287	tracer mass (ug)	0,299
Dispersivity (cm)	8,0	Dispersivity (cm)	13,1	Dispersivity (cm)	24,3
average velocity(cm/min)	1,352				
tot. mass entering tubes(ug)	1,022				

sum of nonlinear square root
0,22

Table 5.1. (continued)

Time,min	**Cmodel, ppb**	**Cexperiment, ppb**	**(Cmodel- Cexperiment)^2**
2	0,6694234	0,71	0,00164646
3,5	0,782206801	0,7	0,006757958
5	0,687238132	0,63	0,003276204
6,5	0,623475382	0,67	0,00216454
8	0,61176791	0,7	0,007784902
9,5	0,629472444	0,67	0,001642483
11	0,656199379	0,71	0,002894507
12,5	0,680641896	0,6	0,006503115
13,5	0,693239699	0,71	0,000280908
14,5	0,702401635	0,63	0,005241997
15,5	0,708236333	0,7	6,78372E-05
17	0,711527246	0,66	0,002655057
18	0,710738682	0,68	0,000944867
19,5	0,706218574	0,68	0,000687414
21	0,69888895	0,68	0,000356792
22,5	0,689828959	0,65	0,001586346
24	0,679829872	0,69	0,000103432
25,5	0,669435684	0,71	0,001645464
27	0,658996051	0,71	0,002601403
28,5	0,648716979	0,75	0,01025825
30	0,638703563	0,66	0,000453538
31,5	0,628993489	0,66	0,000961404
32,5	0,622687454	0,6	0,000514721
33,5	0,616506597	0,59	0,0007026
35	0,607445328	0,66	0,002761994
36	0,601525531	0,6	2,32724E-06
37,5	0,592793502	0,6	5,19336E-05
39	0,584199358	0,55	0,001169596
40,5	0,575702807	0,6	0,000590354
42	0,567269241	0,64	0,005289763
43,5	0,558870319	0,53	0,000833495
45	0,55048394	0,61	0,003542161
46,5	0,542093839	0,53	0,000146261
47,5	0,53649273	0,46	0,005851138
48,5	0,530882858	0,52	0,000118437
50	0,522448946	0,46	0,003899871
51	0,51681296	0,46	0,003227712
52	0,511166541	0,59	0,006214714
54	0,499846035	0,45	0,002484627

Table 5.1 (Continued)

55,5	0,491337127	0,41	0,006615728
57	0,482819432	0,48	7,9492E-06
58,5	0,474300514	0,49	0,000246474
60	0,46578865	0,46	3,35085E-05
61,5	0,457292529	0,45	5,3181E-05
63	0,448821019	0,52	0,005066447
64,5	0,44038297	0,42	0,000415465
66	0,431987062	0,41	0,000483431
67	0,426417359	0,38	0,002154571
68	0,420872519	0,34	0,006540364
69,5	0,41260691	0,46	0,002246105
71	0,404409836	0,44	0,00126666
72,5	0,396288214	0,37	0,00069107
74	0,388248441	0,38	6,80368E-05
75,5	0,38029638	0,39	9,41602E-05
77	0,372437362	0,31	0,003898424
78,5	0,364676192	0,37	2,83429E-05
80	0,357017161	0,35	4,92405E-05
81,5	0,349464065	0,37	0,000421725
83	0,342020222	0,41	0,00462125
84,5	0,334688499	0,34	2,8212E-05
85,5	0,329864193	0,34	0,000102735
86,5	0,325091432	0,35	0,000620437
87,5	0,320370761	0,38	0,003555646
89	0,313388437	0,33	0,000275944
90,5	0,306525667	0,34	0,001120531
92	0,299783427	0,34	0,001617373
93,5	0,293162392	0,3	4,67529E-05
95	0,286662957	0,37	0,006945063
96,5	0,280285263	0,28	8,13751E-08
98	0,274029214	0,27	1,62346E-05
99,5	0,2678945	0,28	0,000146543
101	0,261880617	0,24	0,000478761
102,5	0,255986887	0,24	0,000255581
103,5	0,252124076	0,3	0,002292104
104,5	0,248314012	0,26	0,000136562
106	0,242697129	0,22	0,00051516
107	0,239017519	0,24	9,65268E-07
108	0,235389467	0,2	0,001252414
109,5	0,230043205	0,27	0,001596546

Table 5.1 (Continued)

111	0,224810685	0,26	0,001238288
112,5	0,219690442	0,21	9,39047E-05
114	0,214680939	0,2	0,00021553
115,5	0,209780581	0,2	9,56598E-05
117	0,204987718	0,24	0,00122586
118,5	0,200300657	0,16	0,001624143
119,5	0,197233877	0,19	5,2329E-05
120,5	0,194212832	0,16	0,001170518
122	0,189765871	0,17	0,00039069
123,5	0,185418847	0,15	0,001254495
124,5	0,182575462	0,15	0,001061161
125	0,181169957	0,15	0,000971566
126	0,178390988	0,16	0,000338228
127	0,175654289	0,17	3,1971E-05
128	0,172959322	0,19	0,000290385
128,5	0,171627319	0,19	0,000337555
129	0,170305546	0,19	0,000387872
129,5	0,168993937	0,15	0,00036077
130,5	0,166400939	0,26	0,008760784
131,5	0,163847786	0,17	3,78497E-05
132,5	0,161333944	0,21	0,002368385
133	0,160091597	0,21	0,002490849
134	0,157635719	0,15	5,83042E-05
135	0,155217819	0,15	2,72256E-05
136	0,152837371	0,13	0,000521546
136,5	0,151661027	0,15	2,75901E-06
137	0,150493848	0,15	2,43886E-07
138	0,14818673	0,19	0,00174835
139	0,145915498	0,1	0,002108233
140	0,143679637	0,1	0,001907911
140,5	0,142574812	0,12	0,000509622
141	0,141478638	0,12	0,000461332
141,5	0,140391053	0,12	0,000415795
142	0,139311993	0,1	0,001545433
143	0,137179201	0,1	0,001382293
144	0,135079765	0,15	0,000222613
145	0,133013191	0,19	0,003247496
146	0,130978991	0,19	0,003483479
147	0,128976682	0,18	0,002603379
148	0,127005786	0,19	0,003968271

Table 5.1 (Continued)

149	0,125065829	0,12	2,56626E-05
150	0,123156344	0,12	9,96251E-06
151	0,121276867	0,12	1,63039E-06
152	0,119426941	0,12	3,28397E-07
153	0,117606113	0,19	0,005240875
153,5	0,116706472	0,09	0,000713236
154	0,115813937	0,12	1,75231E-05
154,5	0,114928456	0,09	0,000621428
155	0,114049972	0,12	3,54028E-05
155,5	0,113178431	0,13	0,000282965
156	0,11231378	0,09	0,000497905
157	0,110604932	0,09	0,000424563
158	0,108923002	0,1	7,962E-05
159	0,107267572	0,09	0,000298169
160	0,105638226	0,09	0,000244554
161	0,104034556	0,13	0,000674204
161,5	0,103242223	0,08	0,000540201
162	0,102456159	0,1	6,03272E-06
163	0,100902637	0,1	8,14754E-07
164	0,099373598	0,08	0,000375336
165	0,097868656	0,06	0,001434035
166	0,096387428	0,09	4,07992E-05
167	0,094929539	0,06	0,001220073
168	0,093494619	0,09	1,22124E-05
169	0,092082301	0,09	4,33598E-06
170	0,090692226	0,06	0,000942013
171	0,089324039	0,08	8,69377E-05
172	0,087977391	0,08	6,36388E-05
172,5	0,087312036	0,08	5,34659E-05
173	0,086651937	0,06	0,000710326
173,5	0,085997051	0,09	1,60236E-05
174	0,085347337	0,09	2,16473E-05
174,5	0,084702754	0,08	2,21159E-05
175	0,084063259	0,08	1,65101E-05
176	0,082799371	0,06	0,000519811
177	0,081555351	0,06	0,000464633
178	0,080330879	0,06	0,000413345
178,5	0,079725875	0,08	7,51446E-08
179	0,07912564	0,08	7,64505E-07
180	0,077939326	0,08	4,24638E-06
181	0,07677163	0,08	1,04224E-05

Table 5.1 (Continued)

182	0,075622254	0,06	0,000244055
183	0,074490902	0,07	2,01682E-05
184	0,073377283	0,1	0,000708769
185	0,07228111	0,07	5,20346E-06
186	0,071202103	0,09	0,000353361
187	0,070139984	0,09	0,00039442
188	0,069094479	0,08	0,00011893
189	0,068065321	0,07	3,74298E-06
190	0,067052245	0,07	8,68926E-06
191	0,066054991	0,06	3,66629E-05
191,5	0,065562217	0,05	0,000242183
192	0,065073303	0,08	0,000222806
192,5	0,064588218	0,07	2,92874E-05
193	0,06410693	0,06	1,68669E-05
193,5	0,063629409	0,06	1,31726E-05
194	0,063155624	0,06	9,95796E-06
195	0,06221914	0,08	0,000316159
196	0,061297239	0,07	7,5738E-05
197	0,060389686	0,09	0,000876771
198	0,059496248	0,06	2,53766E-07

CHAPTER 6

RESULTS AND DISCUSSION

The objective of the study is to investigate the applicability of the micro melamine resin as a tracer in geothermal reservoirs. The controlling parameters of the experiments were injection rate, particle size and fracture geometry. The Sigma Inc. gives the guarantee of the stability of melamine resin particles up to 300°C. Thus, the temperature of the experiments was not included in the controlling parameters and the temperature of the system was kept at 80°C.

Injection rate is a critical parameter impacting tracer recovery. In our 5x5x10 cm model experiments, as the injection rate was increased from 15 cc/min to 30 cc/min, the recuperation of the 6 μm fragments expanded from 0.84% to 12.35%. Similar results were obtained for 10 μm and 4 μm particles (Table 1). Similarly, Vilks and Bachinski (1996), found that below the critical velocity significant retention of micro particles was observed due to gravity settlement [38]. Gravitational sedimentation is perceived to be a noteworthy flitration instrument of particles in fractures, particularly for heavy particles. If the conditions are ideal for attachment, gravity segregation and related settling velocity will make the particles to be in motion crosswise over streamlines until the point when they achieve solid surface and settle on it. Both gravitational sedimentation and particle transport by diffusion are function of fluid velocity. By expanding flow rates settled particles might be remobilized [29]. Reimus (1995) found that gravitational settling, fluid advection, and, to minor degree, matrix diffusion to be the representing system of particle transportation in fractures [37]. Micro melamine resin particles' density is 1.51 g/cm^3, which is higher than water density. Therefore, it was found that in order to minimize gravity related particle settlement, the injection rate should be larger than 15 cc/min.

Particles' physical straining is specifically identified with the particle size and shape in respect to the size and geometry of fracture. At fractures with small apertures clogging could happen inside the fracture. Particles moving between fractures can likewise be captured physically in the adjacent rock matrix, given that particles could attach to rock matrix if their size is larger than surrounding fracture openings. This situation results in dead ends keeping subsequent particles from further movement. On the other hand, if particle size is smaller than fracture openings, particles can go inside the reservoir [50; 52; 53].

Table 6.1: Recovery of particles in 5x5x10 cm block dimensions

Size (µm)	**Rate (cc/min)**	**Recovery (%)**	**First arrival time(min)**
4	15	2.62	1.36
6	15	0.84	1.36
6	30	12.35	0.68
10	15	1.67	1.36
10	45	3.57	0.45

The recovery of the micro tracers decreased as the particle size increased. Significant particles trapping was experienced for 4 µm, 6 µm and 10 µm particles in the system that consisted of 5x5x10 cm blocks. Coagulated particles up to a length of 66 µm were observed (Figure 6.1). There was no identifiable peak concentration due to particle trapping in the small fractures and the concentration of particles fell below the measurement limits in a short time (Figure 6.2, Figure 6.3, Figure 6.4). Therefore, mean arrival time could not be calculated. However, when the same experiments were conducted in the system that consisted 5x10x10 cm blocks, it was seen that the recuperation of the particles significantly improved (Table 6.2). This indicates that the fracture aperture and particle size are the key parameters that limit the recovery of the particles.

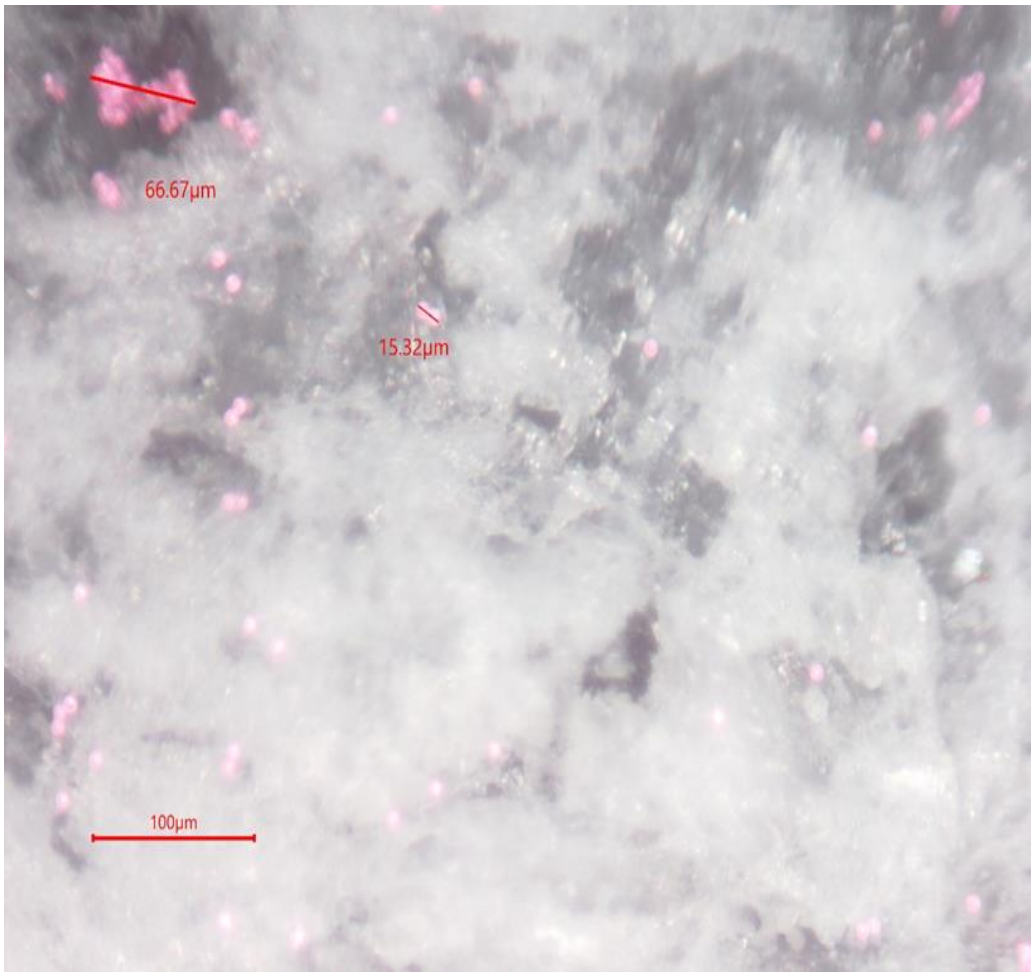

Figure 6.1 Flocculation of the melamine resin particles

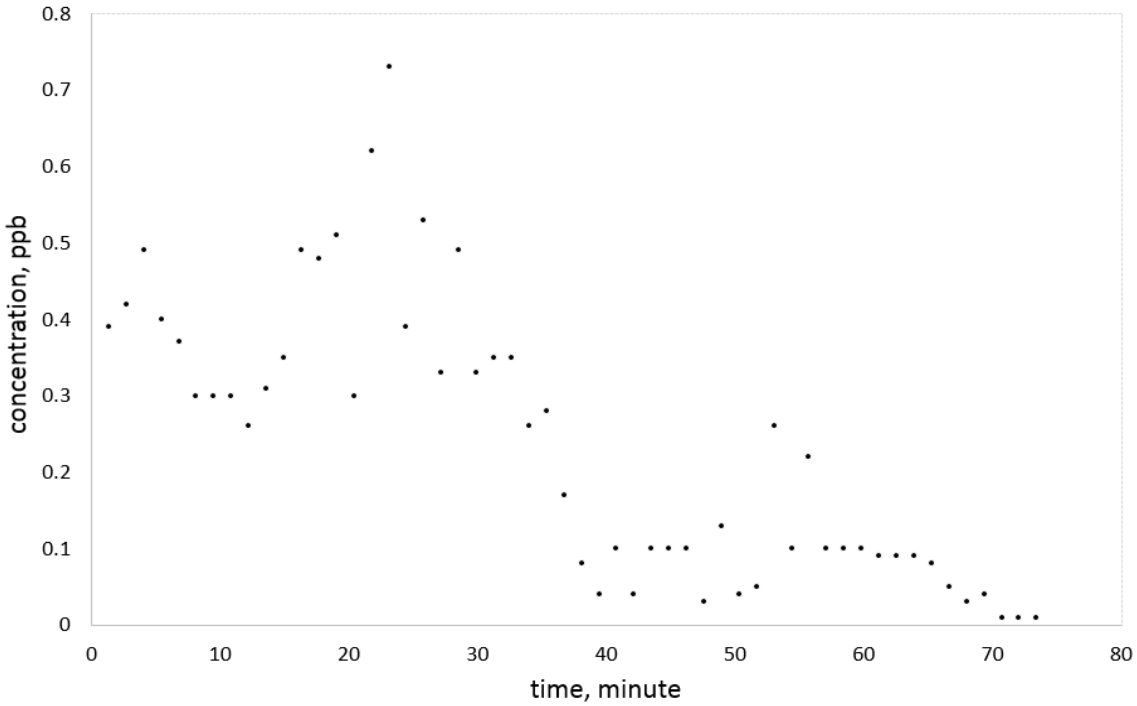

Figure 6.2 Tracer return curve of 4 μm particles with 15 cc/min rate in 5x5x10 cm dimensions of blocks

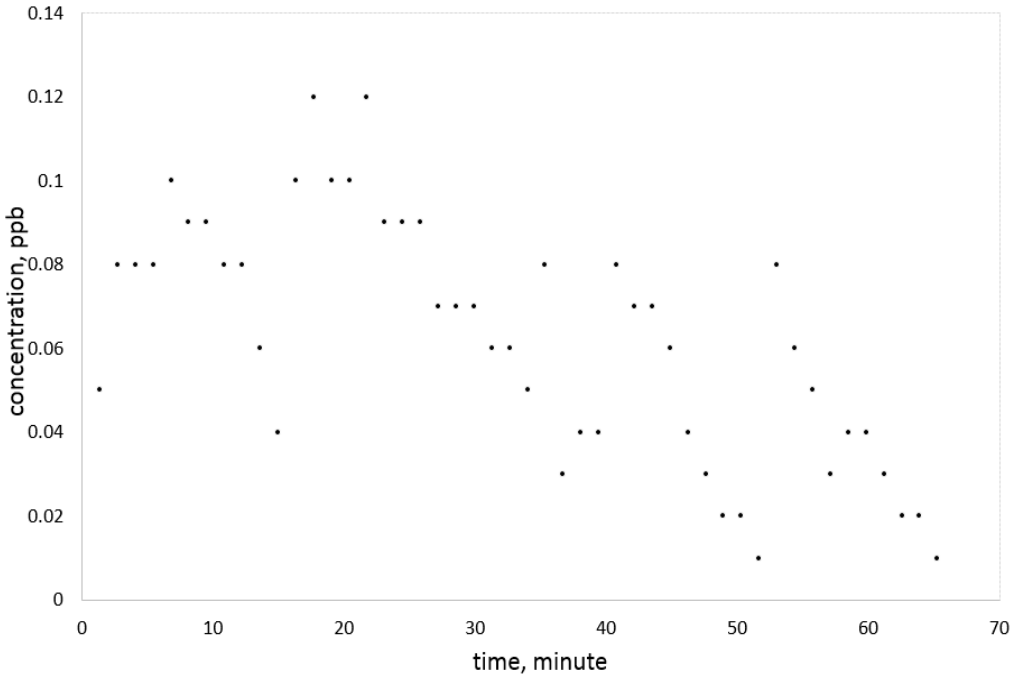

Figure 6.3 Tracer return curve of 6 μm particles with 15 cc/min rate in 5x5x10 cm dimensions of blocks

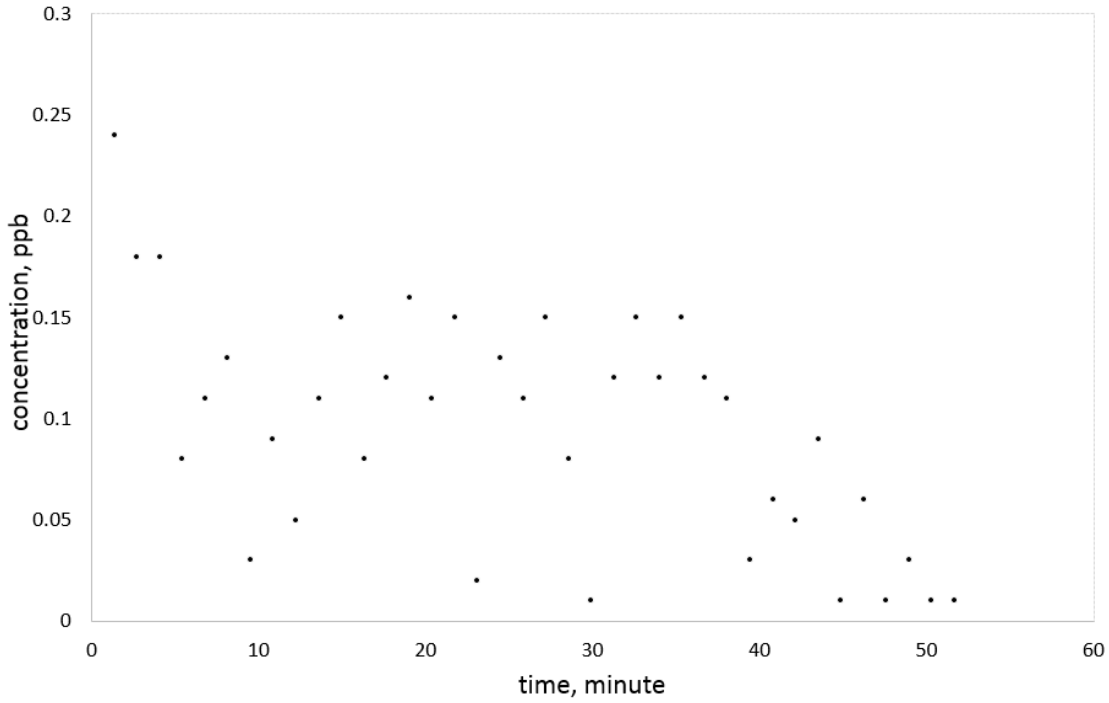

Figure 6.4 Tracer return curve of 10 μm particles with 15 cc/min rate in 5x5x10 cm dimensions of blocks

Table 6.2: Recovery of particles in 5x10x10 cm block dimensions

Dimension of Blocks 5x10x10				
Size (μm)	**Rate (cc/min)**	**Recovery (%)**	**First arrival time(min)**	**mean arrival time(min)**
4	15	38.71	1.5	102.35
6	15	21.49	2	97.30
10	15	17.5	2	82.00

Another purpose of the study is to find out the similarities and differences between conventional rhodamine B and micro melamine resin particles. Therefore, the tracer return curves of the micro tracers and conventional rhodamine-B were matched with the flow models that are described in Akin (2001) (Figure 6.5, 6.6, 6.7, 6.8, 6.9). By minimizing the sum of the square differences, multi-fracture model was best matched with tracer experiment data (Figure 6.9). Once a good match was obtained, reservoir model parameters were then determined using corresponding equations (Table 6.3). It was found that the Peclet numbers were higher than 1 for all the tracers, which corresponded to an advection dominant system. Rhodamine B tracer return curves' dispersion was smaller compared to that of micro melamine resin particles. This suggests that conventional rhodamine B may not find time to leave the high conductive channels and enter several secondary fractures. However, since the density of micro particles are higher than that of the water, there may be a chance for micro particles to enter more fractures compared to rhodamine B so, recovery of rhodamine B is much higher than melamine resin (Table 6.4). It was also observed that first arrival time of melamine resin particles was 4 times less than that of conventional rhodamine-B. Similarly, Bales et al., (1989) reported that the transport of bacteriophages in fractured porous tuff was three times faster than conventional tracer [9].

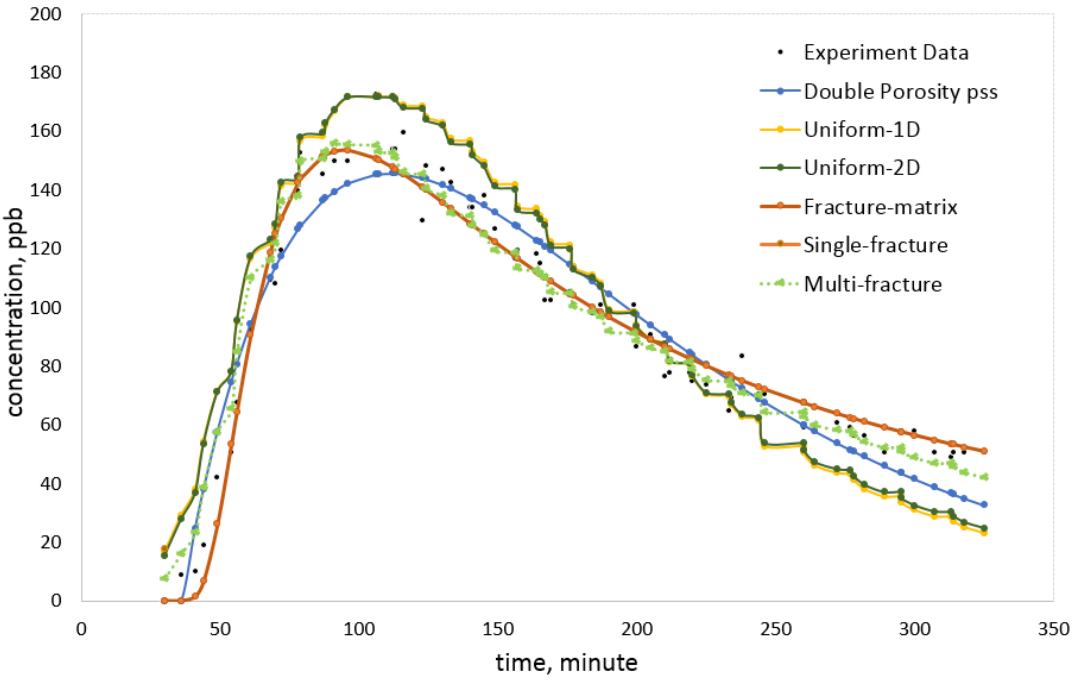

Figure 6.5 Comparison of models to experiment rhodamine-B in 5x10x10 cm dimensions return curve at 5 cc/min

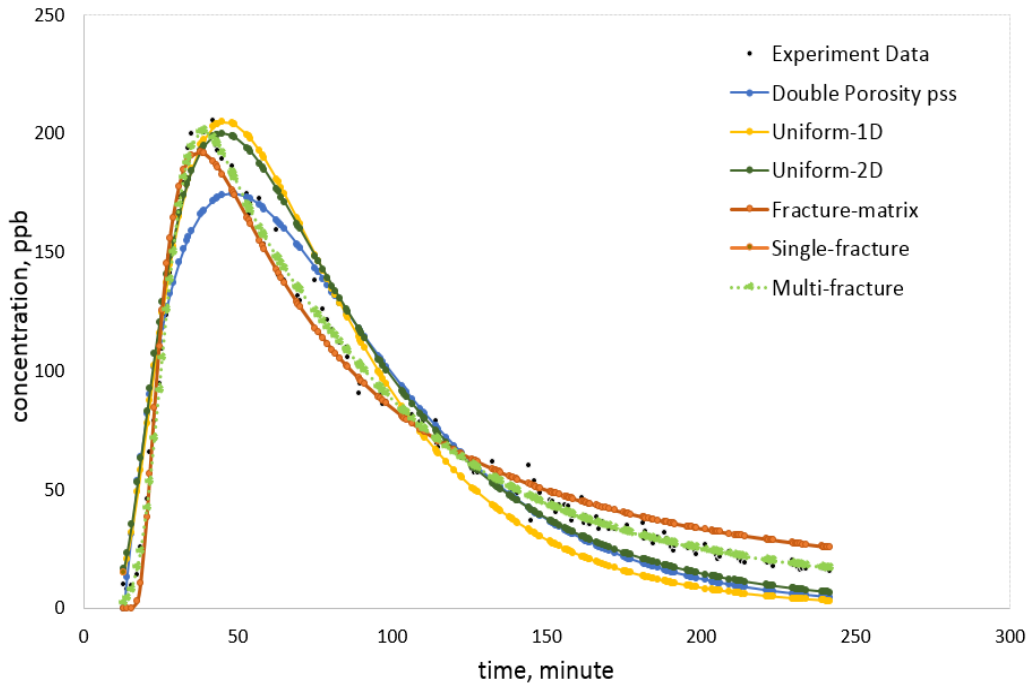

Figure 6.6 Comparison of models to experiment rhodamine-B in 5x10x10 cm dimensions return curve at 15 cc/min

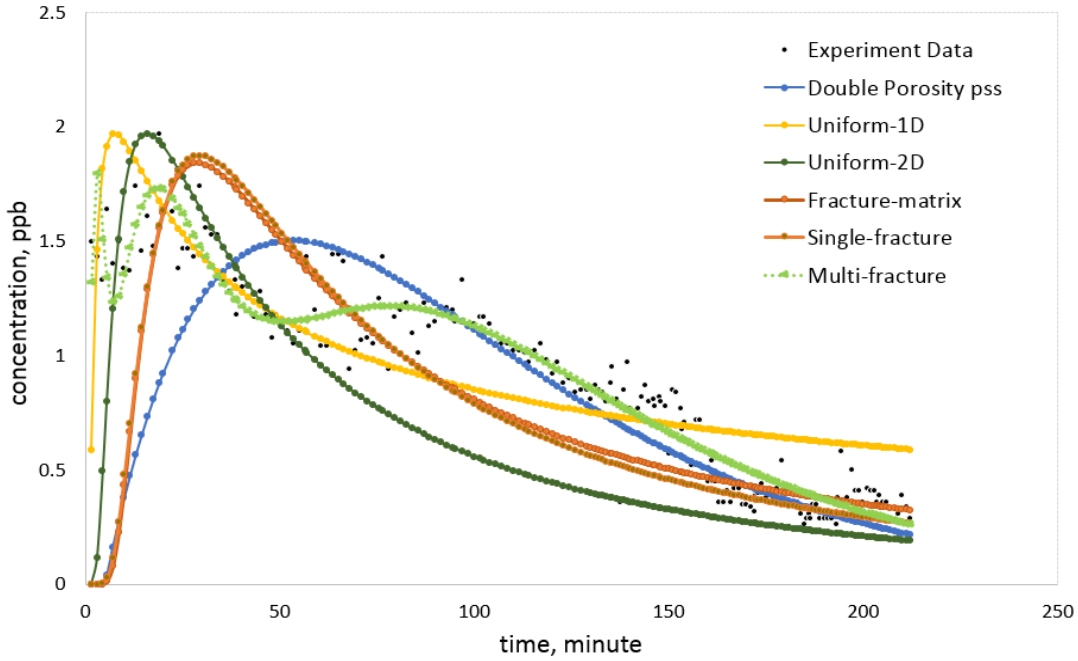

Figure 6.7 Comparison of models to experiment 4 µm particle in 5x10x10 cm dimensions return curve at 15 cc/min

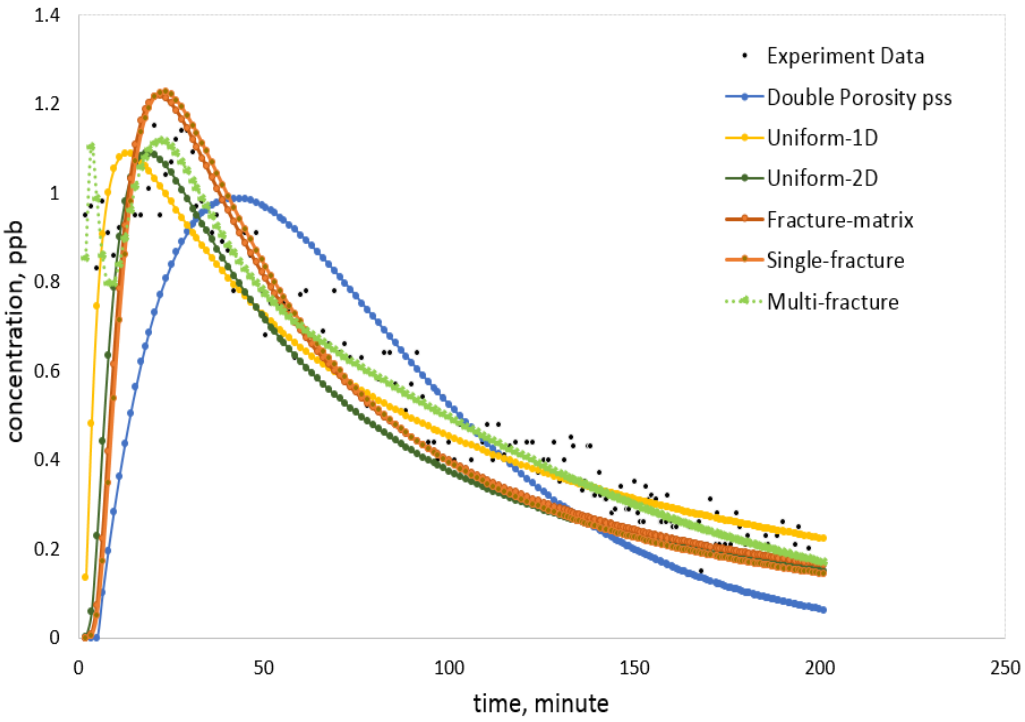

Figure 6.8 Comparison of models to experiment 6 µm particle in 5x10x10 cm dimensions return curve at 15 cc/min

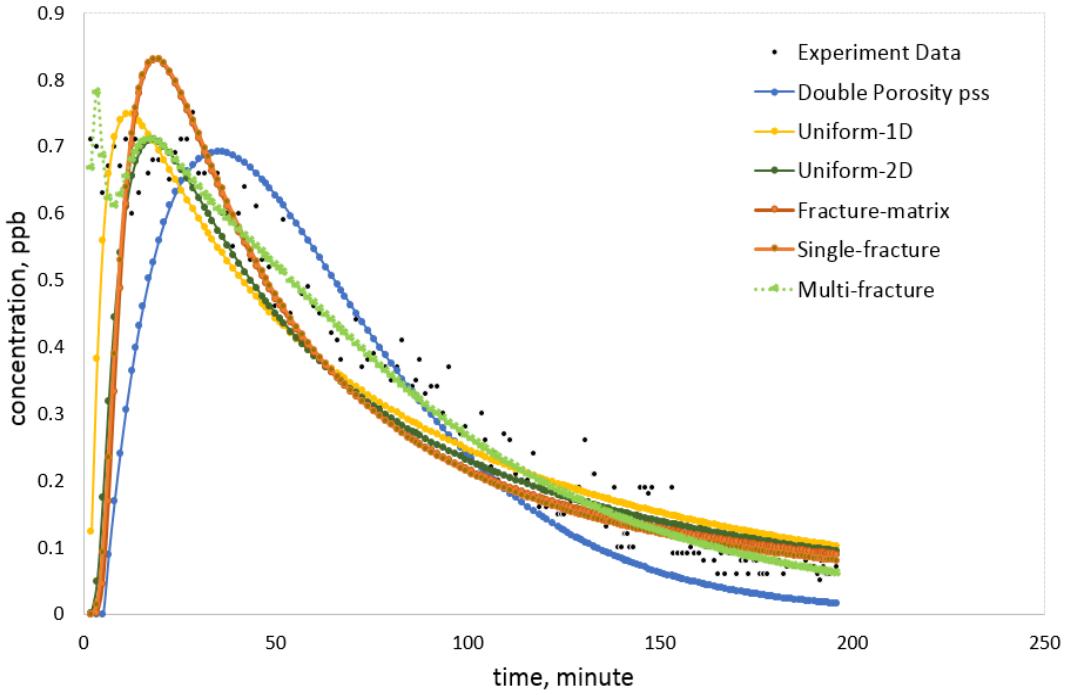

Figure 6.9 Comparison of models to experiment 10 µm particle in 5x10x10 cm dimensions return curve at 15 cc/min

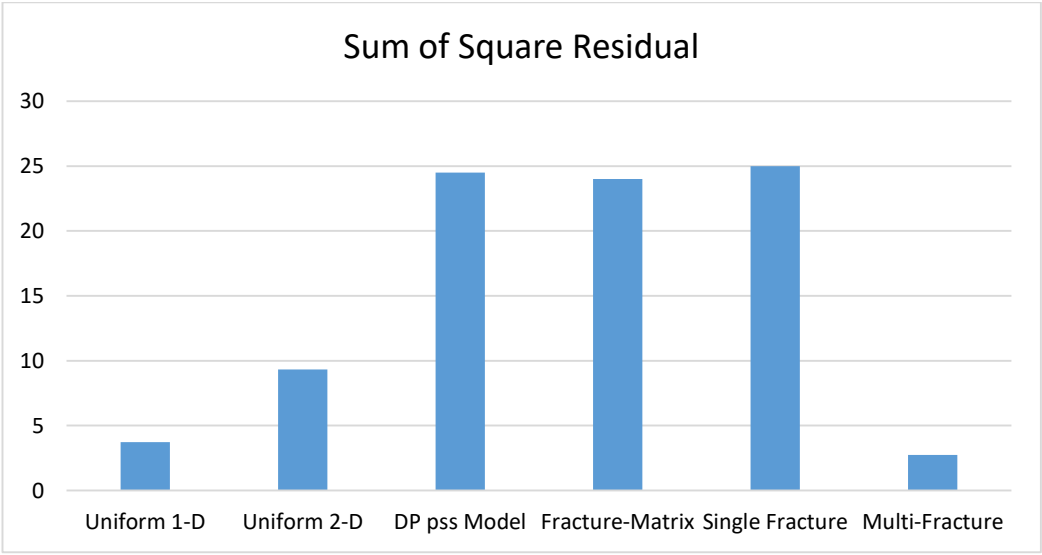

Figure 6.10 Sum of squares residual for different models of 4 µm particle with 15 cc/min rate in 5x10x10 cm dimensions

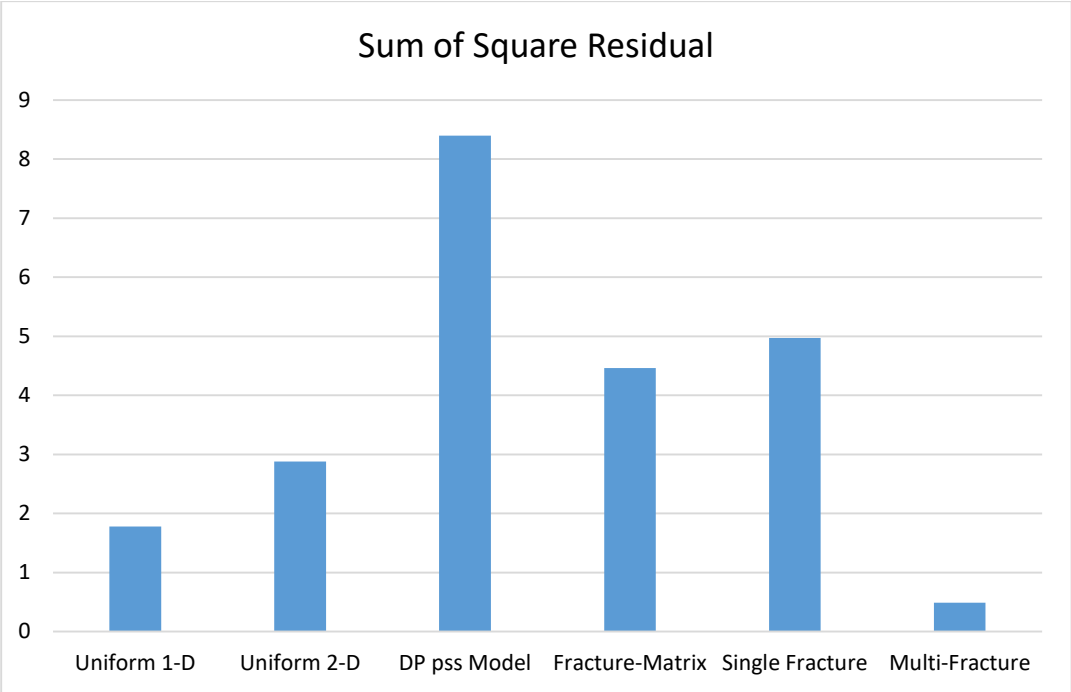

Figure 6.11 Sum of squares residual for different models of 6 µm particle with 15 cc/min rate in 5x10x10 cm dimensions

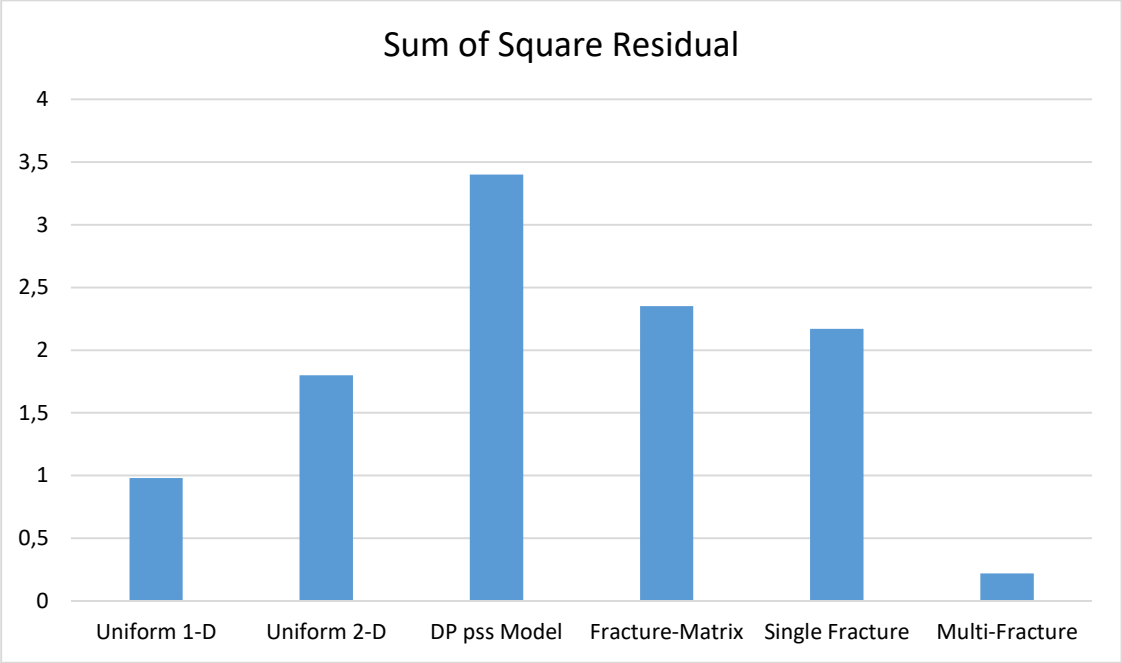

Figure 6.12 Sum of squares residual for different models of 10 µm particle with 15 cc/min rate in 5x10x10 cm dimensions

Table 6.3: Results of Multi-fracture Model

Tracers	Pe	J	t_m(min)	e	m(ug)	DL(cm^2 min^{-1})	u(cm min^{-1})
Rhodamine-B 15 cc/min	24.7	538.80	38.0	0.4701	34	1.5	0.98
	2.40	208005	164.0	0.0009	180	3.5	0.23
	7.80	437.9	76.0	0.520	80	2.4	0.50
4 µm 15 cc/min	8.07	7.96	135.9	0.5314	1.85	1.28	0.28
	3.17	17065.4	49.0	0.00016	1.15	9.06	0.77
	1.44	1.85	11.6	0.4668	0.26	84.17	3.23
6 µm 15 cc/min	5.35	2.76	160	0.551	0.89	1.64	0.23
	3.72	14796	51.44	0.00013	0.77	7.35	0.73
	1.38	1.29	15.26	0.4484	0.20	66.78	2.46
10 µm 15 cc/min	4.68	1.49	117.31	0.5745	0.46	2.56	0.32
	2.86	14105	50.20	0.00007	0.44	9.80	0.75
	1.55	0.99	12.54	0.42344	0.13	72.53	2.99

Table 6.4: Recovery of conventional rhodamine B in 5x10x10 cm block dimension

Rhodamine-B Dimension of Blocks 5x10x10				
Concentration (ppm)	**Rate (cc/min)**	**Recovery (%)**	**First arrival time (min)**	**mean arrival time (min)**
10	5	52.93	29	258
10	15	98.54	9.5	102.7

By using moment analysis method with equations (2.26-2.27), tracer return curves were analyzed. Figure 6.13 shows the flow-storage capacity of the micro particles and rhodamine B. It was observed that rhodamine B is closer to 45° line (homogeneous fractures) compared to micro particles and 4 μm particle size curve is closer to that of rhodamine-B. Lorentz and the Dkystra-Parsons coefficients calculated by equation (2.28-2.29) are two different measures of heterogeneity that are used to quantify the reservoir flow path heterogeneity [49]. As it is mentioned in Shook and Forsmann, Lorentz coefficient varies between 0 and 1[54]. The larger the Lorentz coefficient value, the more heterogeneous the flow paths are. In our experiments, Lorentz coefficient increases with increasing particle size. Rhodamine-B has the smallest Lorentz coefficient, which means that the reservoir open to flow is more homogeneous compared to that of the micro particle flow paths. Dkystra-Parsons coefficient values are similar for the micro particles, however rhodamine-B has different flow paths (Table 6.5). Figure 6.14 shows a plot of interstitial velocity obtained from the slope of figure 6.13 and storage capacity. The curves of micro particles have an inflection at the same point but with a different magnitude of interstitial velocity. This means that micro tracers travel through the same paths, however due to transport mechanisms the magnitudes of the interstitial velocity are not the same. Rhodamine-B has an interstitial velocity somewhat smaller than that of the micro particles, however they become identical as the storage capacity increases. It was also observed that interstitial velocity at the production side is several orders higher than the average velocity of the tracers presented in Table 6.3. This suggests that as the drainage distance of the production well increases the velocity of the flow decreases.

Table 6.5: Heterogeneity of tracers

	Lorenz Coefficient	Dykstra-Parsons Coefficient	Mean Residence Time (min)	Pore Volume cm^3
Rhodamine-B	0.281	0.547	102.7	1440
4 µm particle	0.356	0.334	102.35	465.9
6 µm particle	0.376	0.335	97.3	307
10 µm particle	0.381	0.393	82	210

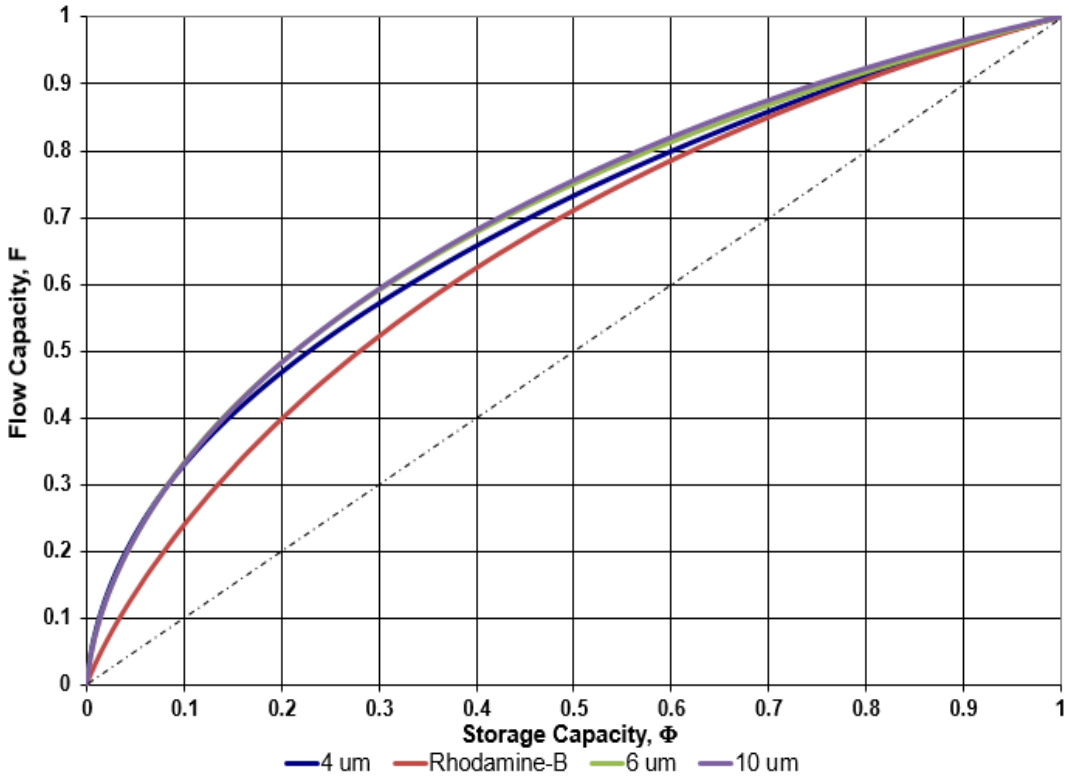

Figure 6.13 Flow geometry of the tracers in 5x10x10 dimensions of blocks

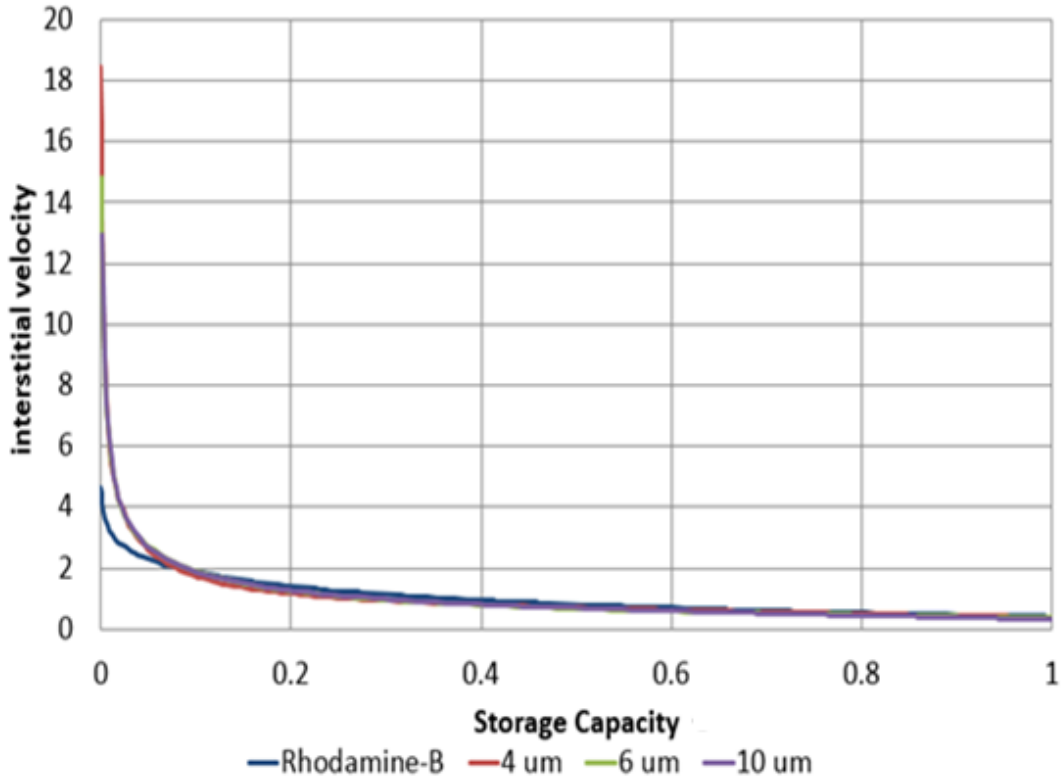

Figure 6.14 Interstitial velocity of the tracers in 5x10x10 dimensions of blocks

Another aim of this study is find out the effect of colder injection on temperature. Temperature recordings showed that due to density differences, temperature of the system was not uniformly distributed at initial state. Colder water was accumulated at the bottom of system and temperature change observed in vertical direction (Fig. 6.15.). Continous injection of cold water cooled the system in a very short time period. Early temperature breakthrough was experienced in all sections of the 2D system in less than 5 minutes. However, rate of cooling was different for temperature recording locations because of the dominant conductive flow paths and the density differences of water (Fig. 6.14.). It was observed that as injection rate increased, temperature reduction accelerated (Fig. 6.15.). The deeper sections of the system experienced larger temperature decrease. The shallower fractures showed less temperature decline rate compared to deep fractures which can be associated with gravity. It was also observed that as the distance from the injection port increased, the rate of cooling decreased.

Due to micro particles plugging, flow directions changed. Thus, some parts of the system warmed because of pluging and fractures that was not prefered by cold water started to experience cooling effect because of changed flow direction (Fig. 6.18-6.19 and 6.20.).

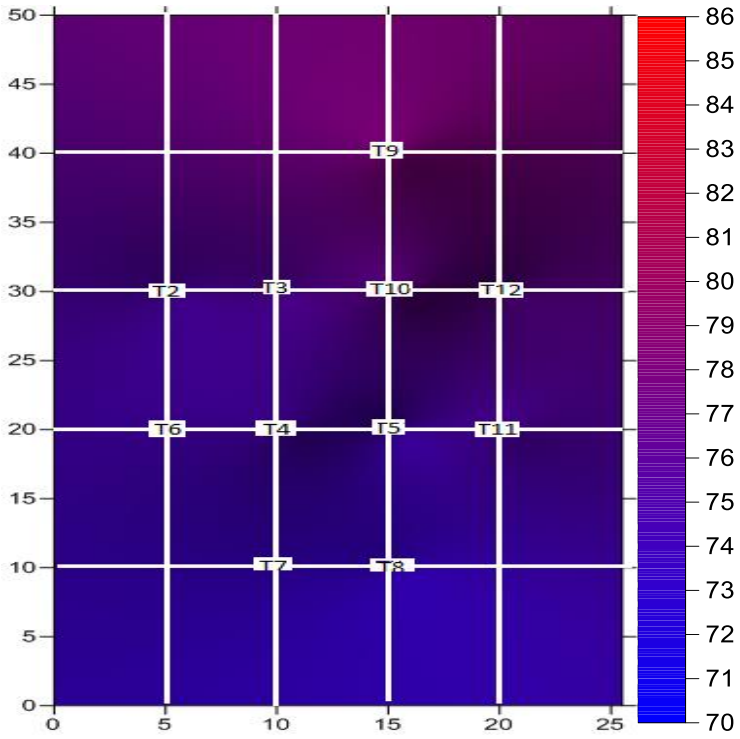

Fig. 6.15 Temperature distribution for the initial state of the system

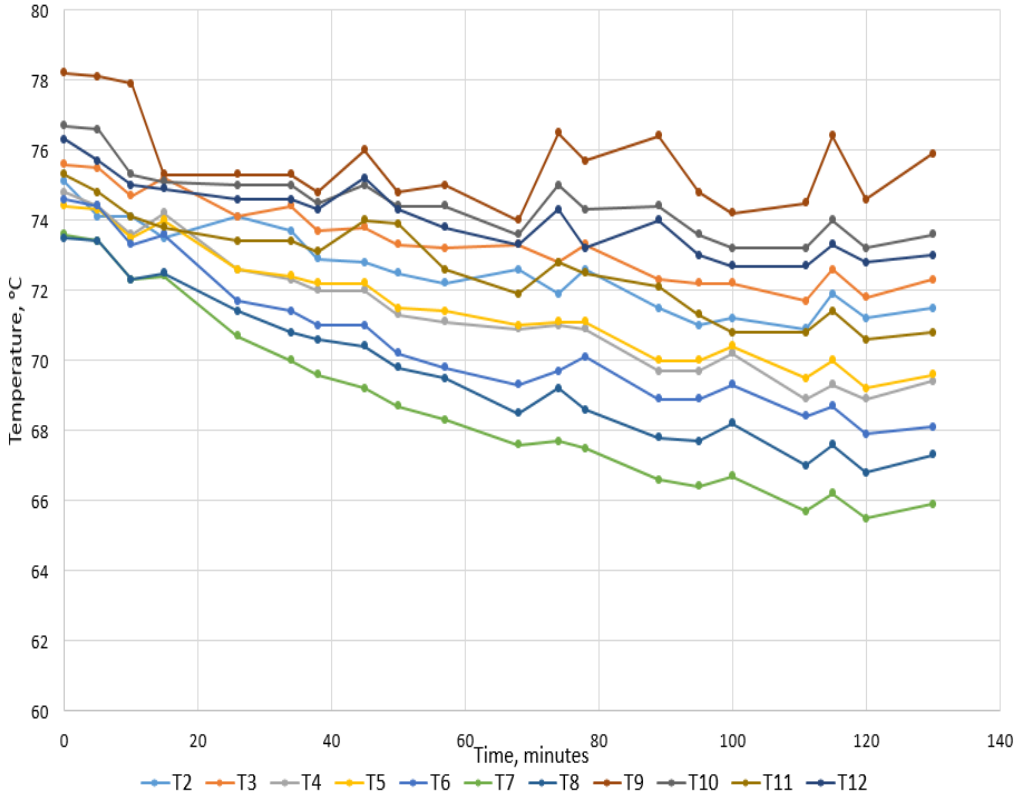

Fig.6.16 Temperature decline during 15cc/min injection rate

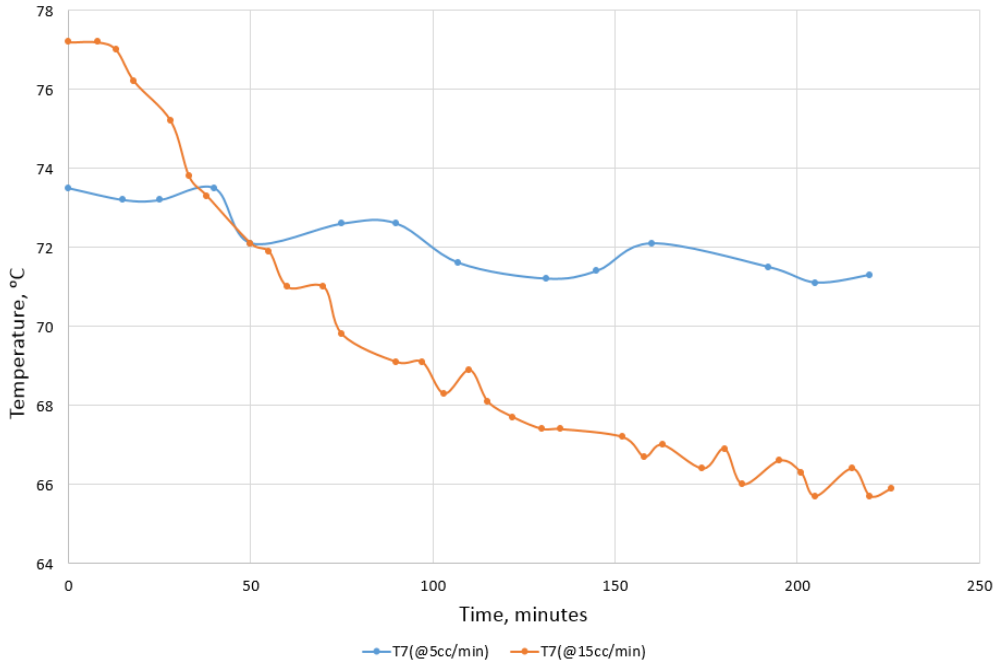

Fig. 6.17 Temperature decline at the location of T7 for different rates

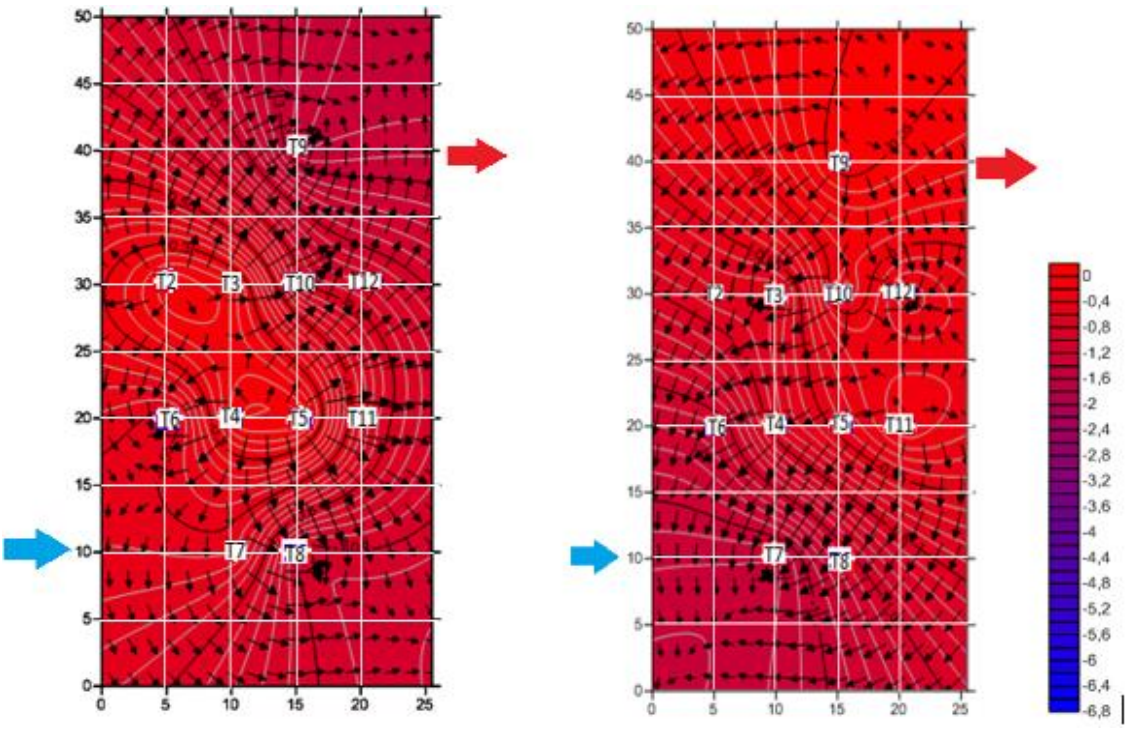

Fig. 6.18 ΔT (Ti- To) at 12.minute and 17. minute in 5x5x10 cm dimensions with 6 µm particles

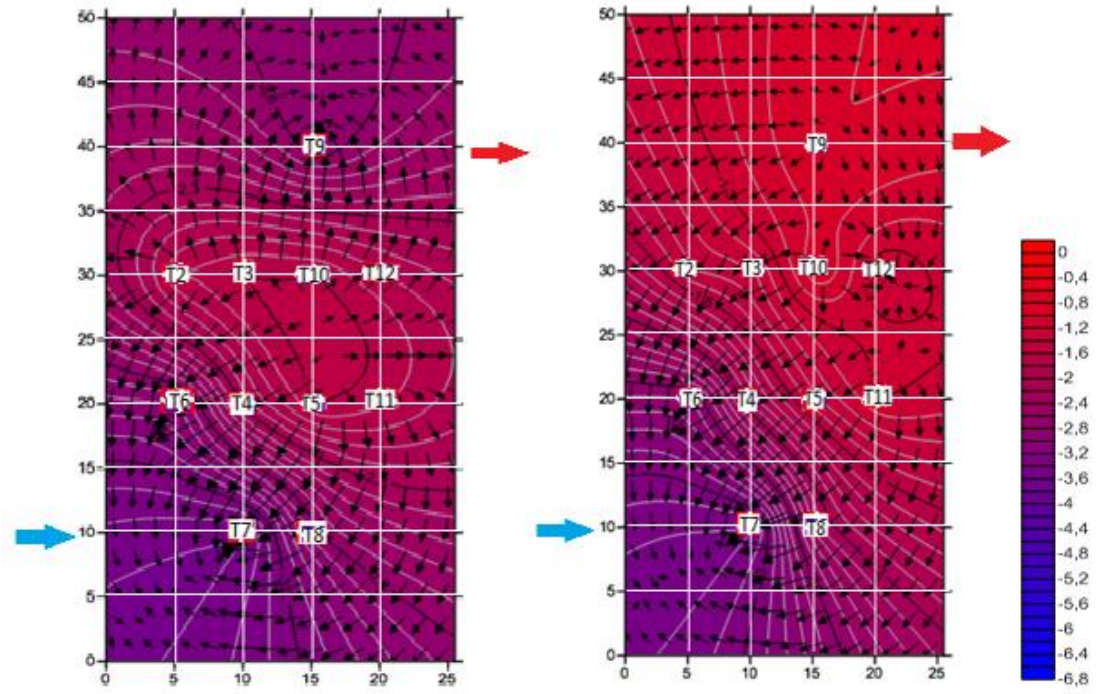

Fig. 6.19 ΔT (Ti- To) at 32. Minute and 37. minute in 5x5x10 cm dimensions with 6 µm particles

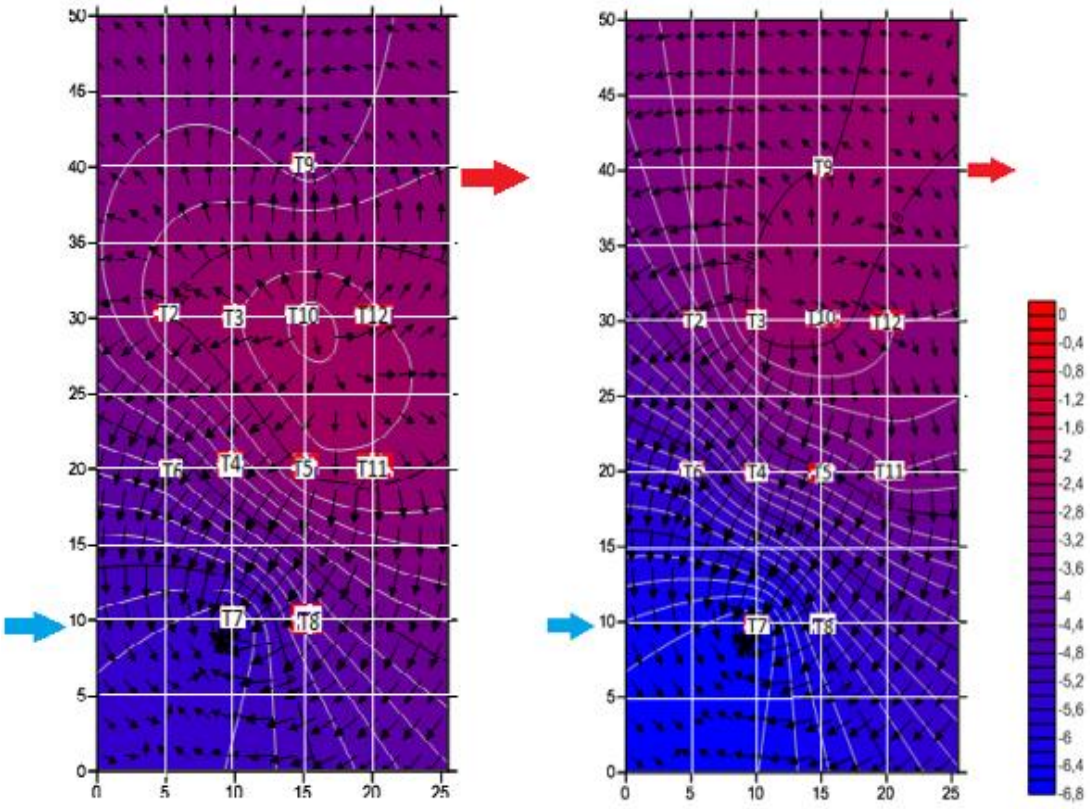

Fig. 6.20 ΔT (Ti- To) at 52.minute and 77.minute in 5x5x10 cm dimensions with 6 µm particles

CHAPTER 7

CONCLUSION

Usually geothermal fluid is produced from natural fractured reservoirs by means of dominant flow paths in it. Contribution of these flow paths are important for understanding dispersion, Peclet number, fracture aperture, fracture permeability etc. In order to better understand fluid flow geometry in an interconnected fracture system, conventional tracer and micro tracer (Micro Particles Based on Melamine Resin Rhodamine B Marked**)** tests are conducted and compared in a laboratory set up, which represent a low entalphy liquid dominated geothermal reservoir. The laboratory model was designed for both conventional tracer and micro tracer in such a way that conventional tracer or micro tracer solution is injected as a slug into deep port of the system which represent deep injection well. Effluent was produced from the shallow port of the system representing production well. As a result, conventional and micro tracer experiments the following conclusions have been reached:

- Microsphere melamine resin particles have been successfully used as micro tracers to identify interconnectivity of fractures in a low enthalpy experimental geothermal reservoir model.
- Both conventional rhodamine-B and micro particles have advection dominant flow
- Dispersion of conventional tracer is smaller than that of micro tracers
- Fracture geometry, injection rate and particle size are critical parameters affecting recovery
- Injection rates should be high enough to prevent particles trapping

- It was found that the recovery of the micro particles increased with increasing flow rate.
- The particle size has an inverse relation with particle recovery.
- Tracer return curve and flow characteristic of 4 μm particle (the smallest one) was similar to conventional rhodamine-B.
- The first arrival time of the micro particles was 4 times faster than that of the conventional rhodamine B.
- It was concluded that physical mechanism controlling flow of the micro particles is an important property that can be used to characterize fractures

CHAPTER 8

RECOMMENDATIONS

Experimental conditions must be enhanced and some part of the equipment used in the set up must be renewed for enhanced experimental monitoring. For example, AB-100 Type scanner and the Turner Quantech Digital Filter Fluorometer used in the set up is quite old. Using new data loggers and fluoremeters will give better results.

This experimental study considers only two type orientations and geometry of the fractures. Different orientation and geometry may end up different results. Hence, in order to acquire a general closure to the problem of reinjection, different models and geometries should be tested.

In this experimental study, back pressure was not used but if back pressure was used it would have given similar result like reservoir conditions.

The micro tracers are very expensive. For example, 5 ml of micro particles based on melamine resin rhodamine B marked (10 μm) is 443 EURO. Therefore, only 0.15 ml of 4 μm, 6 μm and 10 μm micro particle size was used in this experiment. Then, it is recommended that using various types of micro particle size with enough volume will give more information about reservoir parameters.

REFERENCES

1. Falcone, G., Witt, G.J., *Worldwide classification and reporting requirements for geothermal resources, SPE 146435,* (2011)

2. Wilson, B., *Taking the Temperature of Earth's Core,* Science for the Curious Discover Magazine (2014).

3. Axelsson, G.,: *Tracer tests in geothermal resource management*. Proceedings of Tracer 6 – International Conference on Tracers and Tracing Methods, Oslo, Norway, 8 pp.(2011).

4. Zhang, Yuran., Manley, T.S., Li, K., Horne, R.N.: *DNA-Encapsulated Silica Nanoparticles Tracers for Fracture Characterization*, Geothermal Resources Council Transactions, Vol.39, (2015).

5. Rose, P., Riasetto, D., Siy, Jacqueline., Bartl, M., Reimus, P., Mella, M., Leecaster, K., and Petty, S.: *Quantum Dots As Tracers in Geothermal and EGS Reservoirs. Proceedings,* Thirty-Sixth Workshop on Geothermal Reservoir Engineering, Stanford University, (2011).

6. Sigma-Aldrich Inc. Retrieved from: https://www.sigmaaldrich.com/life-science/biochemicals/biochemical-products.html?TablePage=15929463 Accessed on: 05.06.2018

7. American Heritage Dictionary of the English Language. Retrieved from (Accessed on 25 June 2018): https://ahdictionary.com/word/search.html?q=tracer

8. Boyes W., *Instrumentation Reference Book: Edition 3,* pp. 523, (2002)

9. Bayar M, *Tracer Testing in a Fractured Geothermal Reservoir Model,* Master's Thesis, 1987.

10. Alaskar, M. *In-Situ Multifunctional Nanosensors for Fractured Reservoir Characterization.* PhD thesis, Stanford University, (2013).

11. Vetter, O., Zinnow, K., *Evaluation of well to well tracers for geothermal reservoirs*, Geoth. Res. Eng. Man. Prog., Earth Science Division, Lawrence Berkeley Laboratory, Univ. Of California, August

12. Davis, R., *Tracers in Hydrology,* Groundwater, 123-132, Feb.1985

13. Gaspar, W. and Oncescu, M., *Radioactive Tracers in Hydrology*, Elsevier, Second Edition, 1972.

14. Brigham, W., Abbassadeh-Deghani, M., *Analysis of well to well tracer flow to determine reservoir layering*, JPT, 1753-1762, Oct., 1984.

15. Edison, J., *Radioactive tracers used to locate loss circulation*, World oil, 138(7), 197-204, (1954)

16. Howell, L.G. and Frosch, A. ‘’Detection of Radioactive Cements in Cased Wells’’ Trans. AIME, vol.136, 71-78, 1940.

17. Lund, J., Bjelm, L., *Charecteristics, Development and Utilization of Geothermal Resources-a Nordic Perspective,* (2008)

18. Dickson, M.H. and Fanelli, M., 1995, Geothermal Energy, Unesco Energy Engineering Series, John Wiley& Sons, New York.

19. Robinson, B. A., and J. W. Tester, *Dispersed Fluid Flow in Fractured Reservoirs: An Analysis of Tracer-Determined Residence Time Distributions*, *Journal of Geophysical Research,* Vol. 89,No. B12, pp. 10374–10384, (1984).

20. Barker, B.J., Koenig, B.A., and Stark, M.A., 1995: *Water injection management for resource maximization: observations from 25 years at*

The Geysers, California. Proceedings World Geothermal Congress 1995, Florence, Italy, 1959–1964.

21. Axelsson, G., : *Management of geothermal resources. Proceedings of "Workshop for Decision Makers on the Direct Heating Use of Geothermal Resources in Asia"*, organized by UNU-GTP, TBLRREM and TBGMED, Tianjin, China, 15 pp.(2008b)

22. Horne, R., *Reservoir engineering aspects of reinjection*, Geothermics, 449-457, 1985

23. GreenFire Energy Inc. Retrieved From: *http://www.greenfireenergy.com/geothermal-technologies-compared.html* (Accessed on 25 June 2018)

24. McCabe, W. J., Barry, B. J., and Manning, M.R., *Radiotracers in Underground Geothermal Water Flow Studies*, Geothermics, Vol.12, 83-110, 1983

25. Nakamuro, H., *Development and Utilization of Geothermal Energy in Japan*, GRC, Transactions, Vol.5, 33, 1981.

26. Gudmundsson, J. S., *Injection and Tracer Testing in Svartsengi Field of Iceland, Proceeding,* 6th New Zealand Geothermal Workshop, Auckland, N.Z, Nov. 7-9, 1984.

27. Sigma-Aldrich Inc. Retrieved from: https://www.sigmaaldrich.com/content/dam/sigmaaldrich/articles/biofiles/biofiles-pdf/fluorescent-microparticles.pdf (Accessed on: 05.06.2018)

28. Knapp, R. B., Chiarapa, M. L., and Durham, W. B.. *An Experimental Exploration of the Transport and Capture of Abiotic Colloids in a Single Fracture*. Water Resour. Res., 36, 3139-3149, (2000).

29. Wei, Z., Xiangyu, T., Weisbrod, N., and Zhuo, G.. *Review of colloid transport in fractured rocks.* Journal of Material Science, 9, 770-787, (2012).

30. Harton, A. D.. *Influence of Flow Rate on Transport of Bacteriophage in a Column of Highly Weathered and Fractured Shale.* MS Thesis, University of Tennessee, Knoxville, (1996).

31. Hinsby, K., McKay, L. D., Jorgensen, P., Lenczewski, M., and Gerba, C. P.. *Fracture Aperture Measurements and Migration of Solutes, Viruses, and Immiscible Creosote in a Column of Clay-Rich Till. Ground Water*, 34 (6), 1065-1075, (1996).

32. McCarthy, J. F., McKay, L. D., and Bruner, D. D., *Influence of Ionic Strength and Cation Charge on Transport of Colloidal Particles in Fractured Shale Saprolite*. Environ. Sci. Technol., 36, 3735- 3743., (2002).

33. McKay, L. D., Gillham, R. W., and Cherry, J. A. *Field Experiments in a Fractured Clay Till: 2. Solute and Colloid Transport.* Water Resour. Res., 29, 3879-3890, (1993b).

34. Smith, M. S., Thomas, G. W., White, R. E., and Ritonga, D. *Transport of Escherichia Coli Through Intact and Disturbed Soil Columns*. Journal of Environmental Quality, 14 (1), 87-91, (1985).

35. Bales, R.C., Gerba, C.P., Grondin, G.H., and Jensen, S.L.: *Bacteriophage Transport in Sandy Soil and Fractured Tuff.* Appl. Environ. Microbiol., 55, 2061-2067, (1989).

36. Champ, D. R., and Schroeter, J., *Bacterial Transport in Fractured Rock- A Field-Scale Tracer Test at the Chalk River Nuclear Laboratories*. Water Sci. Technol., 20, 81-87, (1988).

37. Reimus, P. W., *The Use Synthetic Particles in Tracer Transport Experiments in Saturated Rock Fractures.* LA-13004-T, Los Alamos National Laboratory, Los Alamos, NM., (1995).

38. Vilks, P., Bachinski, D.B.: *Particle and suspended particle migration experiments in a granite fracture*. Journal of Contaminant Hydrology 21, 269-279, (1996).

39. Cumbie, D. H., and McKay, L. D., *Influence of Diameter on Particle Transport in a Fractured Shale Saprolite*. J. Contam. Hydrol., 37 (1-2): 139-157., (1999*).*,

40. Tang, X. Y., and Weisbrod, N., *Colloid-Facilitated Transport of Lead in Natural Discrete Fractures.* Environmental Pollution, 157, 2266-2274., (2009).

41. Zvikelsky, O., and Weisbrod, N., *Impact of Particle Size on Colloid Transport in Discrete Fractures. Water Resour. r*es., 42, W12S08. doi:10.1029/2006WR004873., (2006).

42. Satter, A., *Chemical Transport in Porous Media with Rate Controlled Adsorption and Dispersion,* SPEJ, 129-138, June 1980.

43. Jensen, C. L., and Horne R.N., *Matrix Diffusion and Its Effect on The Modeling of The Tracer Returns From The Fractured Reservoir at Wairakei, New Zealand,* SGP, TR-71, Stanford University, CA, 1983.

44. Sauty, J.P., *An analysis of hydrodispersive transfer in aquifers.* Water Resources Research 16 (1), 145–158, (1980).

45. Fossum, M.P., Horne, R.N.: *Interpretation of tracer return profiles at Wairakei geothermal field using fracture analysis*, Geothermal Resources Council Transactions 6, 261-264, (1982).

46. Akin, S., Okandan, E.: *Reservoir characterization by tracer testing.* Proceedings of the World Geothermal Congress, Florence, Italy, Vol. 2, pp. 1145-1150, 1995. (40)

47. Kaya, T., *Characterization of Kızılcahamam Geothermal Field by Tracer Testing,* Master's Thesis, (2005)

48. Bullivant, D.P., O'Sullivan, M.J., *Matching a field tracer test with some simple models.* Water Resources Research 25 (8), 1879–1891, (1989)

49. Levenspiel, O., , *Chemical Reaction Engineering*, 2nd edition, New York: John Wiley and Sons, Chapter 9., (1972).

50. James, S. C., and Chrysikopoulos, V. C., *Transport of Polydisperse Colloid Suspensions in a Single Fracture.* Water Resources Research, 35(3), 707-718, (1999).

51. Akin, S.: *Analysis of tracer tests with simple spreadsheet models*. Computer and Geosciences, March 2001.

52. Alonso, U., Missana, T., Patelli, A., et al. *Colloid Diffusion in Crystalline Rock: an Experimental Methodology to Measure Diffusion Coefficients and Evaluate Colloid Size Dependence.* Earth and Planetary Science Letters, 259, 372-383, (2007).

53. Oswald, J. G., and Ibaraki, M., *Migration of Colloids in Discretely Fractured Porous Media: Effect of Colloidal Matrix Diffusion*. Journal of Contaminant Hydrology, 52, 213-244., (2001).

54. Shook, G. M., "A Simple, Fast Method of Estimating Fractured Reservoir Geometry from Tracer Tests," *Transactions of the Geothermal Resources Council*, Vol. 27, September 2003

APPENDIX

Table A.1 Experiment Test Data (10 ppm, 5 cc/min, 5x10x10 cm dimensions) with Multi Fracture Models

5x10x10, 10 ppm, 5 cc/min Multi Fracture Model					
Fracture-I		**Fracture-II**		**Fracture-III**	
mean arrival time (min)	94	mean arrival time (min)	300	mean arrival time (min)	141
Pe	18,8	Pe	3,9	Pe	34,0
J	579,5	J	3352	J	588,42
e1	0,620	e2	0,136	e3	0,243
et	1				
Lenght,cm	37,5				
Injection rate,ml/min	5				

Calculations					
mean velocity (cm/min)	**0,40**	**mean velocity (min/cm)**	**0,13**	**mean velocity (min/cm)**	**0,27**
Dispersion coeff. (cm^2/min)	0,8	Dispersion coeff. (cm^2/min)	1,2	Dispersion coeff. (cm^2/min)	0,3
tracer mass (mg)	0,045	tracer mass (mg)	1,04	tracer mass (mg)	0,042
Dispersivity (cm)	2,0	Dispersivity (cm)	9,6	Dispersivity (cm)	1,1
average velocity(cm/min)	0,263				
total mass entering tubes(mg)	0,180				
abs. and decayed mass(mg)	0,079				

sum of nonlinear square root
2261,83

Table A.1 (continued)

Time,min	Cmodel, (ppb)	Cexperiment, (ppb)	(Cmodel-Cexp)^2
36,0	5,24	8,78	12,54283044
41,0	13,42	10,22	10,23957658
44,0	20,84	18,84	3,983709303
49,0	37,06	41,85	22,9040161
54,0	56,68	50,48	38,40727603
56,0	64,97	67,73	7,614629646
61,0	85,55	92,17	43,86871285
68,0	111,19	109,43	3,092274134
70,0	117,44	108	89,17046168
72,0	123,16	119,49	13,4391586
78,0	137,03	139,62	6,709195454
79,0	138,88	152,52	185,92199
87,0	149,66	145,38	18,30955628
88,0	150,56	151,13	0,323263587
91,0	152,78	149,69	9,531071886
96,0	155,05	149,69	28,75793223
106,0	155,57	172,69	293,0962131
107,0	155,39	145,38	100,1328295
112,0	153,94	154	0,003270047
113,0	153,56	154	0,196963192
116,0	152,22	159,75	56,72708138
123,0	148,17	129,56	346,4481729
124,0	147,50	148,25	0,558459787
130,0	143,08	146,81	13,89602042
133,0	140,66	142,5	3,39454278
140,0	134,62	133,87	0,55630975
141,0	133,72	133,87	0,021886769
145,0	130,10	138,19	65,37981086
149,0	126,46	126,68	0,050342898
156,0	120,13	116,62	12,30919143
157,0	119,24	119,49	0,062571489
164,0	113,19	118,06	23,71953033
165,0	112,35	115,18	7,987379849
167,0	110,71	102,24	71,67220692
169,0	109,09	102,24	46,94155992
176,0	103,72	105,11	1,936962304
177,0	102,99	100,8	4,782771043
184,0	98,12	97,93	0,037263027
187,0	96,17	100,8	21,41421881
190,0	94,30	97,93	13,18433061
199,0	89,11	100,8	136,6791478

Table A.1 (continued)

200,0	88,57	86,42	4,619447308
205,0	85,97	90,74	22,74583297
210,0	83,53	76,36	51,34801357
212,0	82,59	77,8	22,91351133
219,0	79,46	77,8	2,744652182
220,0	79,03	74,92	16,87337275
225,0	76,94	73,48	11,9962834
233,0	73,80	64,81	80,73325643
234,0	73,42	69,17	18,02725133
238,0	71,93	83,55	135,0979936
244,0	69,77	70,61	0,704257485
246,0	69,07	70,61	2,368802734
260,0	64,40	67,73	11,10816077
260,0	64,40	59,1	28,05936637
264,0	63,13	66,23	9,635991099
272,0	60,66	60,54	0,013908172
277,0	59,16	59,1	0,003945333
278,0	58,87	56,23	6,958793264
282,0	57,70	56,1	2,566440086
289,0	55,71	50,48	27,374972
295,0	54,06	50,91	9,896740013
295,0	54,06	57,67	13,06165769
300,0	52,71	57,67	24,60579776
307,0	50,88	50,48	0,156154077
313,0	49,35	49,04	0,095300896
314,0	49,10	50,48	1,90893065
318,0	48,11	50,48	5,624290544
325,0	46,42	50,48	16,48535745
332,0	44,79	49,04	18,0979802

Table A.2 Experiment Test Data (10 ppm, 15 cc/min, 5x10x10 cm dimensions) with Multi Fracture Model

5x10x10, 10 ppm, 15 cc/min, Multi Fracture Model					
Fracture-I		**Fracture-II**		**Fracture-III**	
mean arrival time (min)	38	mean arrival time (min)	164	mean arrival time (min)	76
Pe	24,7	Pe	2,4	Pe	7,8
J	538,83	J	208006	J	437,96
e1	0,475	e2	0,001	e3	0,521
et	0,998				
Lenght,cm	37,5				
Injection rate,ml/min	15				

Calculations					
mean velocity (cm/min)	**0,98**	**mean velocity (cm/min)**	**0,23**	**mean velocity (cm/min)**	**0,50**
Disp. coeff. (cm^2/min)	1,5	Disp. coeff. (cm^2/min)	3,5	Disp. coeff. (cm^2/min)	2,4
tracer mass (mg)	0,071	tracer mass (mg)	181,762	tracer mass (mg)	0,144
Dispersivity (cm)	1,5	Dispersivity (cm)	15,4	Dispersivity (cm)	4,8
average velocity(cm/min)	0,566				
tot. mass entering tubes(mg)	0,289				

sum of nonlinear square root
2576,97

Time, min	**Cmodel, ppb**	**Cexperiment, ppb**	**(Cmodel-Cexperiment)**
13	2,532293738	9,82	53,11066257
14	4,217485591	8,18	15,70152044
15,5	8,244498891	9,33	1,178312658
17,5	17,53192764	14	12,47451288
18,5	24,26391145	25,79	2,328946258
20,5	42,24883129	46,23	15,84970428
21,5	53,34524589	65,72	153,1345393
23	72,02873296	79,04	49,15786556
24,5	92,2173776	94,53	5,348222382
25,5	105,9246209	109,13	10,27445489
27	125,9896452	123,35	6,967726879
28	138,5888095	141,16	6,611020749
29	150,2740036	155,09	23,19382145
31	170,2221109	173	7,716668037

Table A.2 (continued)

32,5	181,8324213	179,23	6,772596544
33,5	187,9399683	177,68	105,2669493
34	190,516472	193,64	9,756427179
35	194,7560364	200,17	29,31100234
38	201,015516	200,95	0,004292342
38,5	201,260068	193,64	58,06543638
39	201,3149293	200,65	0,442130994
42	198,4412541	205,33	47,45482071
43	196,5711784	194,81	3,101749503
43,5	195,5165354	192,77	7,543456737
45	191,9886087	189,36	6,909583729
48	183,981434	186,05	4,278965386
48,5	182,5935534	181,77	0,678240228
49	181,2024792	183,23	4,110840641
53	170,293651	174,75	19,85904623
53,5	168,9854847	165,8	10,14731264
54	167,6933471	170,67	8,860462685
57	160,2957155	172,42	146,9982751
58	157,965521	153,43	20,57095081
58,5	156,8248834	153,14	13,57836549
62,5	148,2290296	159,37	124,121221
63	147,213186	140	52,03005209
64	145,2149149	139,61	31,41507125
65	143,2578993	138,05	27,12221483
69	135,7716177	135,81	0,001473204
69,5	134,8680062	131,52	11,20914523
70	133,9704787	129,48	20,16439899
75	125,2807836	138,05	163,0528876
76	123,5966393	123,93	0,111129388
77,5	121,1000745	125,88	22,84768808
79	118,6378078	121,5	8,192144475
80,5	116,209037	117,21	1,00192697
81,5	114,6083258	114,97	0,130808247
83	112,2350506	111,76	0,225673105
85	109,1232402	109,71	0,344287095
85,5	108,3548274	105,92	5,928384296
89	103,0860764	90,44	159,9232493
89,5	102,3495142	94,72	58,20948685
90	101,6170776	102,22	0,363515375
91	100,1647071	95,22	24,45012828
95,5	93,84102583	99,98	37,6870038
96	93,16031432	89,75	11,63024378
97	91,81229568	86,05	33,2040515

Table A.2 (continued)

98	90,48225832	87,22	10,64232934
103	84,10488103	91,21	50,48271552
103,5	83,49228988	84,2	0,500853618
104	82,8842754	81,87	1,028754596
104,5	82,28083462	79,92	5,573540082
106,5	79,91270687	81,48	2,456407761
109	77,05461711	78,36	1,704024496
110	75,94284827	78,95	9,042961554
110,5	75,39365053	73,88	2,291137916
114	71,67248225	78,95	52,96226466
114,5	71,15825904	69,5	2,749823054
115	70,64831649	67,56	9,537698726
117,5	68,16201537	70,09	3,717124722
120	65,77918145	67,94	4,669136819
122	63,94525445	64,73	0,615825586
122,5	63,4965961	64,43	0,871242838
126	60,46289301	58,4	4,255527576
126,5	60,04443874	56,94	9,637539912
127	59,62963149	59,38	0,062315882
127,5	59,2184424	56,94	5,191299753
132,5	55,29917717	61,92	43,8352949
133	54,92587596	52,66	5,134193883
133,5	54,55584569	55,29	0,538982552
134	54,18905766	51,98	4,87993574
134,5	53,82548326	50,32	12,28841289
135	53,46509397	54,12	0,428901911
138	51,36806064	51,39	0,000481336
138,5	51,02917705	49,93	1,208190193
139	50,69325427	50,91	0,04697871
140	50,03018143	46,62	11,62933735
140,5	49,70297687	48,28	2,024863159
144	47,49090351	60,06	157,9821865
145	46,88327953	36,79	101,8742916
146	46,28612016	53,73	55,41134713
146,5	45,99140153	51,59	31,34430484
147,5	45,40956166	48,67	10,63045816
148	45,12239109	48,37	10,54696362
151	43,45033488	45,65	4,838526634
151,5	43,17993212	43,6	0,176457028
152	42,91183109	44,97	4,236059272
152,5	42,64600897	42,14	0,256045077
153	42,38244313	40,49	3,581340993
154	41,86199072	43,41	2,396332719

Table A.2 (continued)

156	40,8471872	43,25	5,773509354
156,5	40,59879808	40,49	0,011837022
157	40,35249125	43,02	7,11560294
157,5	40,10824584	40,39	0,079385408
158	39,86604118	37,08	7,762025436
158,5	39,62585679	39,12	0,25589109
161,5	38,2260538	46,52	68,78954353
162	37,99945416	36,01	3,957927851
162,5	37,77471789	38,93	1,334676753
163	37,55182624	37,47	0,006695533
163,5	37,33076063	35,52	3,278854046
164	37,11150267	35,52	2,53288075
166	36,25218609	38,15	3,601697641
167	35,83290912	33,57	5,120757675
168	35,42036852	36,59	1,368037806
169	35,01442944	35,42	0,164487475
170	34,61495984	33,28	1,782117781
172	33,8349145	33,2	0,403116417
175	32,71022159	32,8	0,008060162
175,5	32,52787446	33,67	1,304450746
176	32,34694631	34,74	5,72670594
176,5	32,16742301	32,99	0,676632901
177	31,98929057	32,31	0,102854542
181	30,61267255	35,91	28,06167807
181,5	30,44645286	29,1	1,812935317
182	30,28149225	32,31	4,114843707
183	29,95529876	30,46	0,254723343
184	29,63399452	28,02	2,604978308
184,5	29,47514596	27,44	4,141819087
186	29,00567414	29,78	0,599580541
188	28,39579247	31,63	10,46009834
188,5	28,24611962	28,22	0,000682235
189	28,09754416	29,29	1,421950938
190	27,80364302	26,76	1,089190752
190,5	27,65829647	25,59	4,277850299
191	27,51400555	24,03	12,13829467
191,5	27,3707601	26,17	1,441824812
195,5	26,26125202	26,07	0,036577334
196	26,12697723	25,3	0,683891335
196,5	25,9936524	26,08	0,007455907
197	25,86126857	25,59	0,073586637
198	25,59928846	23,45	4,619440894
198,5	25,46967473	22,67	7,838178598

Table A.2 (continued)

201,5	24,71072602	26,86	4,619378656
203,5	24,22200136	24,03	0,036864524
204	24,10190276	23,64	0,213354161
204,5	23,98262187	23,94	0,001816624
205	23,86415118	22,18	2,836365211
205,5	23,74648327	20,62	9,774897668
206	23,6296108	21,5	4,535242161
209	22,94467896	23,84	0,80159976
211	22,50307626	22,86	0,127394559
211,5	22,39449145	22,47	0,005701541
212	22,28662002	21,7	0,344123053
212,5	22,17945562	20,72	2,13001071
213	22,07299195	19,75	5,396291598
214	21,86214199	19,16	7,301571317
221	20,45999772	19,45	1,020095389
221,5	20,36454776	18,97	1,944763463
222	20,26969633	20,72	0,202773392
222,5	20,17543832	20,14	0,001255874
223	20,08176865	18,58	2,255309086
223,5	19,98868234	17,8	4,790330377
229,5	18,91539737	20,28	1,862140326
230	18,8294627	18	0,688008374
230,5	18,74404666	18,87	0,015864245
231	18,65914497	18,87	0,044459842
231,5	18,57475343	17,22	1,835356858
232	18,49086785	16,34	4,626232521
233	18,3245981	16,73	2,54274311
234	18,16030318	16,83	1,769706539
239	17,36735798	16,97	0,15789336
239,5	17,29058917	16,44	0,723501941
240	17,21426511	16,8	0,17161558
240,5	17,13838228	16,83	0,095099631
241	17,06293723	15,95	1,238629267
241,5	16,98792651	15,37	2,617686195

Table A.3 Experiment Test Data (4 μm, 298 ppb, 15 cc/min, 5x10x10 cm dimensions) with Multi Fracture Model

5x10x10, 298 ppb, 4μm, 15cc/min, Multi Fracture Model					
Fracture-I		**Fracture-II**		**Fracture-III**	
mean arrival time (min)	136	mean arrival time (min)	49	mean arrival time (min)	12
Pe	8,1	Pe	3,2	Pe	1,4
J	7,9616672	J	17065,4372	J	1,85
e1	0,5314328	e2	0,00016087	e3	0,467
et	0,9983985				
Lenght,cm	37,5				
Injection rate,ml/min	15				

Calculations					
mean velocity (cm/min)	**0,28**	**mean velocity (cm/min)**	**0,77**	**mean velocity (cm/min)**	**3,23**
Dispersion coeff. (cm^2/min)	1,3	Dispersion coeff. (cm^2/min)	9,1	Dispersion coeff. (cm^2/min)	84,2
tracer mass (ug)	3,4760491	tracer mass (ug)	7141,00105	tracer mass (ug)	0,559
Dispersivity (cm)	4,6	Dispersivity (cm)	11,8	Dispersivity (cm)	26,1
average velocity(cm/min)	1,4237064				
total mass entering tubes(ug)	3,2569297				

sum of nonlinear square root
2,75

Time,min	**Cmodel, ppb**	**Cexperiment, ppb**	**(Cmodel-Cexperiment)^2**
1,5	1,321565312	1,5	0,031838938
3,0	1,795264327	1,43	0,133418029
4,5	1,506232229	1,33	0,031057799
5,5	1,340166704	1,64	0,089900005
7,0	1,233178171	1,4	0,027829523
8,5	1,261471273	1,5	0,056895954
10,0	1,357596727	1,38	0,000501907
11,5	1,47059897	1,37	0,010120153
13,0	1,572179677	1,74	0,028163661
14,5	1,650135775	1,46	0,036151613
16,0	1,701497219	1,61	0,008371741

Table A.3 (continued)

17,5	1,727896271	1,48	0,061452561
19,0	1,732902596	1,97	0,056215179
20,0	1,726388161	1,73	1,30454E-05
22,5	1,684244543	1,63	0,00294247
24,0	1,646493733	1,38	0,07101891
25,0	1,618025409	1,47	0,021911522
26,5	1,57224903	1,47	0,010454864
28,0	1,524667005	1,43	0,008961842
29,5	1,47701996	1,74	0,069158502
31,0	1,430680035	1,56	0,016723653
32,5	1,386696103	1,53	0,020536007
34,0	1,345836419	1,53	0,033916225
35,5	1,308628476	1,33	0,000456742
37,0	1,275396041	1,28	2,11964E-05
38,5	1,246293289	1,33	0,007006813
39,0	1,237516231	1,18	0,003308117
40,5	1,213924367	1,3	0,007409015
42,0	1,194331566	1,25	0,003098975
43,5	1,178534175	1,17	7,28321E-05
45,0	1,166271408	1,28	0,012934193
46,5	1,157243091	1,18	0,000517877
48,0	1,151124587	1,08	0,005058707
49,0	1,148496019	1,18	0,000992501
50,5	1,146477376	1,13	0,000271504
52,0	1,14646959	1,11	0,001330031
53,5	1,148146671	1,05	0,009632769
55,0	1,151197553	1,11	0,001697238
56,5	1,155329684	1,11	0,00205478
57,0	1,156899759	1,43	0,074583742
59,0	1,163891769	1,2	0,001303804
60,5	1,169640583	1,04	0,016806681
62,0	1,175585919	1,04	0,018383541
63,5	1,18154012	1,44	0,06680151
65,0	1,187337825	1,44	0,063838175
66,5	1,192835022	1,41	0,047160628
68,0	1,197907887	0,94	0,066516478
69,5	1,202451482	1,02	0,033288543
71,0	1,206378379	1,07	0,018599062
72,5	1,209617237	1,08	0,016800628
74,0	1,212111387	1,05	0,026280102
75,5	1,213817441	1,25	0,001309178
76,5	1,214500992	1,43	0,046439822
78,0	1,214828952	0,94	0,075530953

Table A.3 (continued)

79,5	1,214307981	1,17	0,001963197
81,0	1,212932345	1,2	0,000167246
82,5	1,210703891	1,23	0,00037234
84,0	1,207631036	1,1	0,01158444
85,5	1,203727851	1,01	0,03753048
87,0	1,199013213	1,23	0,000960181
88,5	1,193510041	1,13	0,004033525
90,0	1,187244606	1,15	0,001387161
91,5	1,180245901	1,18	6,04671E-08
93,0	1,172545091	1,21	0,00140287
94,5	1,164175012	1,2	0,00128343
95,0	1,16124212	1,15	0,000126385
97,0	1,14883054	1,33	0,032822373
98,5	1,138844434	1,13	7,8224E-05
100,0	1,128317192	1,14	0,000136488
101,5	1,117284427	1,17	0,002778932
102,5	1,109665904	1,17	0,003640203
104,0	1,097869093	1,14	0,001775013
105,5	1,085660201	1,04	0,002084854
107,0	1,073073196	1,05	0,000532372
108,5	1,060141253	1,05	0,000102845
110,0	1,046896645	1,02	0,00072343
111,5	1,033370661	1,02	0,000178775
113,0	1,019593538	1,01	9,2036E-05
114,0	1,010283703	0,97	0,001622777
115,5	0,996152205	1,02	0,000568717
117,0	0,981844723	1,05	0,004645142
118,5	0,96738731	0,98	0,00015908
120,0	0,952804831	0,92	0,001076157
121,5	0,938120972	0,97	0,001016272
123,0	0,923358238	0,88	0,001879937
124,5	0,908537972	0,9	7,2897E-05
126,0	0,893680372	0,84	0,002881582
127,5	0,878804507	0,85	0,0008297
129,0	0,863928352	0,85	0,000193999
130,0	0,854019142	0,81	0,001937685
131,0	0,844122086	0,87	0,000669666
132,0	0,834241731	0,85	0,000248323
133,0	0,82438243	0,84	0,000243909
134,0	0,814548339	0,8	0,000211654
135,0	0,804743432	0,88	0,005663551
135,5	0,799853113	0,95	0,022544088
136,5	0,790099025	0,81	0,000396049

Table A.3 (continued)

137,5	0,780383256	0,36	0,176722082
138,5	0,770709156	0,85	0,006287038
139,5	0,761079907	0,97	0,043647605
140,0	0,756283053	0,77	0,000188155
141,0	0,746726696	0,75	1,07145E-05
142,0	0,73722245	0,77	0,001074368
143,0	0,72777295	0,82	0,008505829
144,0	0,718380687	0,87	0,022988416
145,0	0,70904801	0,8	0,008272265
146,0	0,69977713	0,81	0,012149081
146,5	0,69516552	0,78	0,007196889
147,5	0,685991196	0,82	0,017958359
148,0	0,681428956	0,8	0,014059092
149,0	0,672355442	0,78	0,011587351
150,0	0,663351294	0,57	0,008714464
151,0	0,654418107	0,85	0,038252277
152,0	0,645557363	0,84	0,037807939
153,0	0,636770438	0,77	0,017750116
153,5	0,632405058	0,68	0,002265279
154,0	0,628058602	0,71	0,006714393
155,0	0,619423029	0,48	0,019438781
156,0	0,610864796	0,52	0,008256411
157,0	0,602384886	0,72	0,013833315
158,0	0,593984198	0,72	0,015879982
159,0	0,58566354	0,68	0,008899368
160,0	0,577423643	0,45	0,016236785
161,0	0,569265157	0,54	0,000856449
161,5	0,565216626	0,45	0,013274871
162,0	0,561188658	0,45	0,012362918
163,0	0,55319465	0,36	0,037324173
164,0	0,545283566	0,36	0,03433
165,0	0,537455775	0,41	0,016244975
166,0	0,529711581	0,36	0,028802021
167,0	0,522051227	0,42	0,010414453
168,0	0,514474901	0,42	0,008925507
169,0	0,506982733	0,35	0,024643578
170,0	0,499574799	0,35	0,022372621
171,0	0,492251128	0,34	0,023180406
172,0	0,485011698	0,32	0,027228861
172,5	0,481423555	0,39	0,008358266
173,0	0,477856443	0,4	0,006061626
174,0	0,470785252	0,44	0,000947732
175,0	0,463797972	0,38	0,0070221

Table A.3 (continued)

176,0	0,456894414	0,41	0,002199086
177,0	0,450074346	0,38	0,004910414
178,0	0,443337505	0,42	0,000544639
179,0	0,436683592	0,54	0,01067428
180,0	0,430112276	0,41	0,000404504
181,0	0,423623198	0,25	0,030145015
182,0	0,417215966	0,35	0,004517986
183,0	0,410890166	0,36	0,002589809
184,0	0,404645354	0,31	0,008957743
185,0	0,398481066	0,26	0,019177006
185,5	0,395428966	0,29	0,011115267
186,0	0,392396811	0,31	0,006789235
186,5	0,389384538	0,29	0,009877286
187,0	0,386392081	0,35	0,001324384
188,0	0,380466346	0,35	0,000928198
189,0	0,374619057	0,29	0,007160385
190,0	0,368849648	0,29	0,006217267
191,0	0,363157536	0,29	0,005352025
192,0	0,357542126	0,29	0,004561939
193,0	0,352002804	0,26	0,008464516
193,5	0,349261482	0,38	0,000944857
194,5	0,343835119	0,58	0,055773851
195,0	0,341149917	0,35	7,8324E-05
196,0	0,335835068	0,38	0,001950541
197,0	0,330593741	0,5	0,028698481
198,0	0,325425269	0,41	0,007152885
199,0	0,320328976	0,41	0,008040893
200,0	0,315304179	0,36	0,001997716
201,0	0,310350187	0,42	0,012023082
202,0	0,305466304	0,41	0,010927294
203,0	0,300651828	0,41	0,011957023
203,5	0,298270396	0,36	0,003810544
204,0	0,295906052	0,39	0,008853671
204,5	0,293558704	0,35	0,00318562
205,0	0,291228264	0,36	0,004729552
206,0	0,286617751	0,36	0,005384954
207,0	0,282073795	0,29	6,28247E-05
208,0	0,277595676	0,28	5,78077E-06
209,0	0,273182671	0,31	0,001355516
210,0	0,268834059	0,39	0,014681185
211,0	0,264549113	0,34	0,005692836
212,0	0,260327111	0,29	0,00088048

Table A.4 Experiment Test Data (6 μm, 290 ppb, 15 cc/min, 5x10x10 cm dimensions) with Multi Fracture Model

5x10x10, 290 ppb, 6 μm, 15 cc/min, Multi Fracture Model					
Fracture-I		**Fracture-II**		**Fracture-III**	
mean arrival time (min)	160	mean arrival time (min)	51	mean arrival time (min)	15
Pe	5,3	Pe	3,7	Pe	1,4
J	2,7615325	J	14796,8	J	1,288098
e1	0,5511665	e2	0,000131	e3	0,448403
et	0,9997005				
Lenght,cm	37,5				
Injection rate,ml/min	15				

Calculations					
mean velocity (cm/min)	**0,23**	**mean velocity (cm/min)**	**0,73**	**mean velocity (cm/min)**	**2,46**
Dispersion coeff. (cm^2/min)	1,6	Dispersion coeff. (cm^2/min)	7,3	Dispersion coeff. (cm^2/min)	66,8
tracer mass (ug)	1,6067866	tracer mass (ug)	5850,337	tracer mass (ug)	0,455632
Dispersivity (cm)	7,0	Dispersivity (cm)	10,1	Dispersivity (cm)	27,2
average velocity(cm/min)	1,1400875				
total mass entering tubes(ug)	1,8582713				

sum of nonlinear square root
0,49

Time,min	**Cmodel, ppb**	**Cexperiment, ppb**	**(Cmodel- Cexperiment)**
2,0	0,854118795	0,95	0,009193205
3,5	1,102215882	0,97	0,01748104
5,0	0,987005298	0,83	0,024650663
6,5	0,858422609	0,98	0,014781062
8,0	0,795386448	0,91	0,013136266
9,5	0,796319667	0,86	0,004055185
11,0	0,838036642	0,92	0,006717992
12,5	0,897863638	0,98	0,006746382
14,0	0,959888086	0,98	0,000404489
15,5	1,014873017	0,95	0,004208508
17,0	1,058458403	0,95	0,011763225
18,0	1,080473313	1,09	9,07578E-05
19,0	1,096926492	1,01	0,007556215

Table A4. (continued)

20,5	1,111918252	1,15	0,00145022
22,0	1,116714759	0,95	0,027793811
23,5	1,113115029	1,04	0,005345807
25,0	1,102895514	1,07	0,001082115
26,5	1,087676715	1,12	0,001044795
28,0	1,06886415	1,14	0,005060309
29,5	1,047632885	1,14	0,008531684
31,0	1,024936288	1,09	0,004233287
32,0	1,009370371	0,97	0,001550026
33,5	0,98581722	0,98	3,384E-05
34,5	0,970184748	0,97	3,41318E-08
36,0	0,947112362	0,91	0,001377327
37,5	0,924728344	0,95	0,000638657
39,0	0,90321728	0,89	0,000174696
40,5	0,882692367	0,87	0,000161096
42,0	0,863211683	0,78	0,006924184
43,5	0,844791634	0,8	0,002006291
45,0	0,827417903	0,91	0,006819803
46,5	0,811054226	0,86	0,002395689
48,0	0,795649349	0,91	0,013076071
49,5	0,781142443	0,78	1,30518E-06
50,5	0,771937458	0,68	0,008452496
52,0	0,758778767	0,75	7,70667E-05
53,0	0,750409127	0,69	0,003649263
54,5	0,738408716	0,75	0,000134358
55,5	0,730749362	0,75	0,000370587
57,0	0,719724924	0,74	0,000411079
58,5	0,709204945	0,63	0,006273423
60,0	0,699133605	0,77	0,005022046
61,5	0,689459507	0,78	0,008197581
63,0	0,68013575	0,66	0,000405448
64,5	0,671119874	0,58	0,008302831
66,0	0,662373708	0,69	0,000763212
67,5	0,653863173	0,66	3,76607E-05
69,0	0,645558025	0,78	0,018074645
70,5	0,637431598	0,64	6,59669E-06
72,0	0,629460517	0,66	0,00093266
73,5	0,621624421	0,63	7,01503E-05
75,0	0,613905692	0,51	0,010796393
76,5	0,606289186	0,63	0,000562203
78,0	0,598761986	0,52	0,00620345
79,5	0,591313166	0,52	0,005085568
81,0	0,583933572	0,58	1,5473E-05

Table A4. (continued)

82,5	0,576615619	0,64	0,00401758
84,0	0,569353108	0,64	0,004990983
85,5	0,562141054	0,57	6,1763E-05
87,0	0,554975536	0,51	0,002022799
88,5	0,547853555	0,51	0,001432892
90,0	0,540772909	0,57	0,000854223
91,5	0,533732084	0,64	0,01129287
93,0	0,52673015	0,54	0,000176089
94,5	0,519766677	0,44	0,006362723
96,0	0,51284165	0,44	0,005305906
97,0	0,508246476	0,4	0,0117173
98,5	0,501386409	0,54	0,001491009
100,0	0,494566286	0,44	0,00297748
101,5	0,487787083	0,4	0,007706572
103,0	0,481049936	0,48	1,10236E-06
104,5	0,474356094	0,48	3,18537E-05
106,0	0,467706895	0,4	0,004584224
107,5	0,46110373	0,43	0,000967442
109,0	0,454548025	0,44	0,000211645
110,5	0,448041216	0,48	0,001021364
112,0	0,441584731	0,4	0,00172929
113,5	0,435179978	0,48	0,002008834
115,0	0,428828333	0,41	0,000354506
116,5	0,422531124	0,43	5,57841E-05
118,0	0,41628963	0,44	0,000562182
119,5	0,410105068	0,41	1,10394E-08
121,0	0,403978593	0,44	0,001297542
122,5	0,39791129	0,44	0,00177146
124,0	0,391904172	0,37	0,000479793
125,5	0,38595818	0,4	0,000197173
127,0	0,380074178	0,4	0,000397038
128,5	0,374252959	0,44	0,004322673
130,0	0,368495237	0,35	0,000342074
131,0	0,364692351	0,4	0,00124663
132,0	0,360918144	0,35	0,000119206
133,0	0,357172775	0,45	0,008616894
133,5	0,355310949	0,43	0,005578454
134,5	0,351609098	0,35	2,5892E-06
135,0	0,349769105	0,35	5,33127E-08
136,0	0,34611105	0,33	0,000259566
136,5	0,344293014	0,35	3,25697E-05
137,5	0,340678985	0,43	0,007978244
138,0	0,338883013	0,43	0,008302305

Table A4. (continued)

139,0	0,335313197	0,32	0,000234494
139,5	0,33353937	0,32	0,000183315
140,5	0,330013911	0,37	0,001598887
141,0	0,328262291	0,32	6,82655E-05
142,0	0,324781293	0,31	0,000218487
142,5	0,323051923	0,31	0,000170353
143,5	0,319615451	0,32	1,47878E-07
144,0	0,317908352	0,28	0,001437043
145,0	0,314516432	0,29	0,000601055
145,5	0,31283161	0,32	5,13858E-05
146,5	0,309484234	0,34	0,000931212
147,0	0,307821675	0,31	4,7451E-06
148,0	0,3045188	0,29	0,000210796
148,5	0,302878475	0,29	0,000165855
149,5	0,299620025	0,31	0,000107744
150,0	0,298001888	0,35	0,002703804
151,0	0,294787758	0,28	0,000218678
151,5	0,29319175	0,26	0,001101692
152,5	0,290021805	0,26	0,000901309
153,0	0,28844785	0,34	0,002657624
154,0	0,285321927	0,31	0,000609007
154,5	0,283769938	0,32	0,001312617
155,5	0,280687849	0,31	0,000859202
156,0	0,279157726	0,31	0,000951246
157,0	0,276119258	0,26	0,00025983
157,5	0,274610888	0,26	0,000213478
158,5	0,271615807	0,26	0,000134927
159,0	0,270129068	0,32	0,00248711
160,0	0,267177116	0,26	5,1511E-05
160,5	0,265711874	0,25	0,000246863
161,5	0,262802775	0,25	0,000163911
162,0	0,261358887	0,29	0,000820313
163,0	0,258492346	0,26	2,27302E-06
163,5	0,25706966	0,21	0,002215553
164,5	0,254245365	0,21	0,001957652
165,0	0,25284372	0,25	8,08675E-06
166,0	0,250061343	0,21	0,001604911
166,5	0,248680572	0,28	0,000980907
167,5	0,245939769	0,26	0,00019769
168,0	0,244579697	0,15	0,008945319
169,0	0,241880112	0,21	0,001016342
169,5	0,240540558	0,21	0,000932726
170,5	0,237881821	0,31	0,005201032

Table A4. (continued)

172,0	0,233944329	0,21	0,000573331
172,5	0,232645242	0,28	0,002242473
173,0	0,231352823	0,21	0,000455943
174,0	0,228787903	0,18	0,002380259
174,5	0,227515356	0,21	0,000306788
175,5	0,224989978	0,18	0,002024098
176,0	0,2237371	0,21	0,000188708
177,0	0,221250852	0,18	0,001701633
177,5	0,220017436	0,28	0,003597908
178,5	0,217569899	0,25	0,001051711
179,0	0,216355732	0,18	0,001321739
180,0	0,213946482	0,21	1,55747E-05
180,5	0,212751351	0,23	0,000297516
181,0	0,211562518	0,18	0,000996193
182,0	0,209203645	0,18	0,000852853
182,5	0,208033557	0,18	0,00078588
183,5	0,205711958	0,18	0,000661105
184,0	0,204560397	0,18	0,000603213
185,0	0,202275629	0,18	0,000496204
185,5	0,201142372	0,23	0,000832763
186,0	0,200015168	0,21	9,96969E-05
187,0	0,197778816	0,2	4,93366E-06
187,5	0,196669619	0,2	1,10914E-05
188,5	0,194469056	0,23	0,001262448
189,0	0,19337764	0,18	0,000178961
190,0	0,191212415	0,26	0,004731732
190,5	0,190138555	0,17	0,000405561
191,5	0,188008216	0,17	0,000324296
192,0	0,186951687	0,17	0,00028736
193,0	0,18485578	0,15	0,001214925
193,5	0,183816353	0,21	0,000685583
194,5	0,181754426	0,25	0,004657458
195,0	0,180731874	0,15	0,000944448
196,0	0,178703472	0,18	1,68099E-06
197,0	0,176697166	0,2	0,000543022
198,0	0,174712758	0,15	0,00061072
199,0	0,172750044	0,17	7,56274E-06
200,0	0,170808824	0,17	6,54196E-07
201,0	0,168888898	0,17	1,23455E-06